Ikaros-1 Couples Cell Cycle Arrest of Late Striatal Precursors With Neurogenesis of Enkephalinergic Neurons

Raquel Martín-Ibáñez,[1,2] Empar Crespo,[1,2] Noelia Urbán,[1,2] Solène Sergent-Tanguy,[1] Cristina Herranz,[1,2] Montserrat Jaumot,[1] Manuel Valiente,[3] Jason E. Long,[4] José Ramón Pineda,[1] Celia Andreu,[2,5] John L.R. Rubenstein,[4] Óscar Marín,[3] Katia Georgopoulos,[6] Guadalupe Mengod,[2,7] Isabel Fariñas,[2,5] Oriol Bachs,[1] Jordi Alberch,[1,2] and Josep M. Canals[1,2]*

[1]Departament de Biologia Cellular, Immunologia i Neurociències, Facultat de Medicina, Institut d'Investigacions Biomèdiques August Pi I Sunyer (IDIBAPS), Universitat de Barcelona, E-08036 Barcelona, Spain
[2]Centro de Investigación Biomédica en Red sobre Enfermedades Neurodegenerativas (CIBERNED), 41013 Sevilla, Spain
[3]Instituto de Neurociencias de Alicante, CSIC, and Universidad Miguel Hernández, E-03550 Sant Joan d'Alacant, Spain
[4]Nina Ireland Laboratory of Developmental Neurobiology, Department of Psychiatry, University of California at San Francisco, San Francisco, California 94143
[5]Departamento de Biología Celular, Universidad de Valencia, E-46010 Burjassot, Spain
[6]Cutaneous Biology Research Center, Massachusetts General Hospital, Harvard Medical School, Charlestown, Massachusetts 02114
[7]Department of Neurochemistry and Neuropharmacology, Institut d'Investigacions Biomèdiques de Barcelona-Consejo Superior de Investigaciones Científicas, IDIBAPS, E-08036 Barcelona, Spain

ABSTRACT

During central nervous system development, several transcription factors regulate the differentiation of progenitor cells to postmitotic neurons. Here we describe a novel role for Ikaros-1 in the generation of late-born striatal neurons. Our results show that Ikaros-1 is expressed in the boundary of the striatal germinal zone (GZ)/mantle zone (MZ), where it induces cell cycle arrest of neural progenitors by up-regulation of the cyclin-dependent kinase inhibitor (CDKi) $p21^{Cip1/Waf1}$. This effect is coupled with the neuronal differentiation of late precursors, which in turn is critical for the second wave of striatal neurogenesis that gives rise to matrix neurons. Consistently, *Ikaros*$^{-/-}$ mice had fewer striatal projecting neurons and, in particular, enkephalin (ENK)-positive neurons. In addition, overexpression of Ikaros-1 in primary striatal cultures increases the number of calbindin- and ENK-positive neurons. Our results also show that Ikaros-1 acts downstream of the Dlx family of transcription factors, insofar as its expression is lost in Dlx1/2 double knockout mice. However, we demonstrate that Ikaros-1 and Ebf-1 independently regulate the final determination of the two populations of striatal projection neurons of the matrix compartment, ENK- and substance P-positive neurons. In conclusion, our findings identify Ikaros-1 as a modulator of cell cycle exit of neural progenitors that gives rise to the neurogenesis of ENK-positive striatal neurons. J. Comp. Neurol. 518:329–351, 2010.

INDEXING TERMS: telencephalon; differentiation; striatum; P21; Dlx; Ebf-1

Neural progenitor cells (NPCs) that are located at concrete positions during brain development give rise to different neuronal and glial cell types (Bertrand et al., 2002). These processes are regulated by several proneural transcription factors that follow specific temporal expression patterns and regulate neurogenesis of discrete neuronal populations. Some of these factors are likely to be part of the switch from neurogenesis to gliogenesis, insofar as the

Additional Supporting Information may be found in the online version of this article.

Grant sponsor: Ministerio de Educación y Ciencia; Grant number: BFU2005-04773/BMC (to O.M.); Grant number: SAF2006-05212 (to O.B.); Grant number: SAF2005-01335 (to J.A.); Grant number: SAF2006-04202 (to J.M.C.); Grant sponsor: Ministerio de Sanidad y Consumo [CIBERNED; to I.F., G.M., J.A., E.C.; Red de Terapia Celular (RETICS; to I.F. and J.M.C.)]; Grant sponsor: Fundació La Caixa (to O.M., J.A.); Grant sponsor: European Commission; Grant number: STREP 005139 (INTERDEVO; to O.M.) Grant sponsor: EURYI program (O.M.); Grant sponsor: CIRIT, Generalitat de Catalunya (to N.U.).

Solène Sergent-Tanguy's current address is INSERM U643, Nantes, France. José Ramón Pineda's current address is Institut Curie, CNRS UMR 146, Orsay, France.

*CORRESPONDENCE TO: Dr. Josep M. Canals, Departament de Biologia Cellular, Immunologia i Neurociències, Facultat de Medicina, Universitat de Barcelona, C/Casanova 143, E-08036 Barcelona, Spain.
E-mail: jmcanals@ub.edu

Received 4 March 2009; Revised 24 May 2009; Accepted 31 August 2009.
DOI 10.1002/cne.22215
Published online September 16, 2009 in Wiley InterScience (www.interscience.wiley.com).

TABLE 1.
List of Mutant Mice Used

Gene target	Mutation	Background strain	Reference
Ikaros	Knockout mice involving a deletion of a 1.35-kb genomic fragment encompassing the 59 coding region of exon 7	C57BL/6	Wang et al., 1996
Dlx-5/6	Transgenic mice expressing *cre recombinase* and *EGFP* from a bicistronic construct under the control of the *Dlx-5/6* enhancer element *id6/id5*	C57BL/6	Stenman et al., 2003
Dlx-1/2	Knockout mice with targeted mutagenesis to introduce deletions into the locus of the *Dlx-1* and *-2* genes linked on mouse chromosome 2	C57BL/6	Qiu et al., 1997
Ebf-1	Knockout mice in which 3.4 kb of the mouse *ebf* gene comprising exons 1-3 was replaced with 1.4 kb of the PGK:neo cassette	C57BL/6	Lin and Grosschedl, 1995
P21	Knockout mice generated by replacing the p21 coding sequence with a neomycin-resistance cassette	C57BL/6	Brugarolas et al., 1995

former precedes thefinal differentiation of NPCs to glial cells.

Striatal projection neurons derive from NPCs of the lateral ganglionic eminence (LGE) of the ventral telencephalon (Campbell, 2003). NPCs from the germinal zone (GZ) of the LGE proliferate and multiply and then migrate to the mantle zone (MZ), the striatal primordium, where they undergo terminal neuronal differentiation (Merkle and Alvarez-Buylla, 2006). Two separate waves of neurogenesis generate neurons that will populate distinct striatal anatomical structures: the patches or striosomes and the matrix (van der Kooy and Fishell, 1987). These two compartments of the striatum can be defined on the basis of neuropeptide expression: the patch compartment consists of clusters of substance P (SP)-expressing neurons (Song and Harlan, 1994a), which develop early, and their neurogenesis peaks between E12 and E13 in mice (Mason et al., 2005). In contrast, the matrix compartment contains both enkephalin (ENK)- and SP-positive neurons (Song and Harlan, 1994b) that are generated later, at about E14–E15 in mice (Mason et al., 2005).

The sequential actions of many transcription factors participate in the development of striatal projection neurons (Campbell, 2003). Among them, Gsh1 and -2 and Mash1 appear to be necessary for the generation of early-born striatal neurons (Toresson and Campbell, 2001; Yun et al., 2002, 2003), whereas Dlx-1 and -2 are involved in the neurogenesis of late-born striatal neurons (Anderson et al., 1997; Yun et al., 2002). All these transcription factors are highly expressed in the GZ, and their main function is the maintenance of homeostasis of NPCs. Further transcription factors are expressed in the postmitotic MZ, where they intervene in the final differentiation of striatal neurons. One of these factors is Ebf-1, which in the MZ participates in the development of SP-positive striatal projection neurons located in the matrix compartment (Garel et al., 1999; Lobo et al., 2006).

Another of the factors selectively expressed in the MZ during striatal development is Ikaros (Georgopoulos et al., 1992; Molnar and Georgopoulos, 1994; Willett et al., 2001; Agoston et al., 2007), the founding member of a family that was initially identified as a hematopoietic cell type-specific transcription factor (Georgopoulos, 2002; Yoshida et al., 2006). It has recently been shown that Ikaros family members participate in the development of ENK-positive neurons in the striatum (Agoston et al., 2007). However, the mechanism by which Ikaros is involved in this process is unknown. Here we show that Ikaros-1 participates in cell cycle arrest of late NPCs through the regulation of $p21^{Cip1/Waf1}$ and that this process is linked to the neurogenesis of ENK-positive striatal neurons. We also found that Ikaros-1 acts downstream of the Dlx family of transcription factors but independently of Ebf-1.

MATERIALS AND METHODS

Animal subjects

Mice were maintained under standard conditions, with food and water ad libitum. All animal procedures were approved by local committees, in accordance with European Communities Council Directive 86/609/EU. B6CBA wild-type (wt) mice (from Charles River Laboratories, Les Oncins, France); Dlx-5/6-Cre-IRES-GFP transgenic mice (Stenman et al., 2003); and *Ikaros* (Wang et al., 1996), *Dlx-1/2* (Qiu et al., 1997), *Ebf-1* (Lin and Grosschedl, 1995), and *p21* (Brugarolas et al., 1995) knockout mice (−/−) were used (see Table 1 for details). These strains were maintained by back-crossing to C57BL/6 mice. Genotypes were determined by PCR, as described elsewhere (Lin and Grosschedl, 1995; Wang et al., 1996; Qiu et al., 1997; Jaime et al., 2002; Stenman et al., 2003).

BrdU birth dating and proliferation

The day of pregnancy, determined by the first detection of a vaginal sperm plug in daily inspection, was considered embryonic day (E) 0.5. Pregnant mice were injected intraperitoneally with bromodeoxyuridine (BrdU; 50 mg/kg; Sigma Chemical Co., St. Louis, MO). BrdU was adminis-

tered at E12.5, E14.5, and E16.5, and the embryos were subsequently allowed to develop until E18.5, at which point the dams were terminally anesthetized and the embryos were removed and processed for BrdU immunohistochemistry (see diagram in Supp. Info. Fig. 1). To analyze the proliferation in the GZ in vivo, E14.5 pregnant mice received a single dose of BrdU. Thirty minutes later, they were terminally anesthetized, and the embryos were processed for BrdU immunohistochemistry.

Primary striatal cultures

E14.5 fetal brains were excised, and the LGEs were dissected and dissociated with a fire-polished Pasteur pipette. Cells were plated onto 24-well plates containing glass coverslips precoated with 0.1 mg/ml poly-D-lysine (Sigma Chemical Co.) at a density of 150,000 cells/cm^2. We obtained mixed neuron–glial cultures by growing cells in Eagle's minimum essential medium (MEM; Invitrogen S.A., El Prat de Llobregat, Barcelona, Spain) supplemented with 7.5% fetal bovine serum (FBS; Invitrogen S.A.), 0.6% D-(+)-glucose (Sigma Chemical Co.), and 100 U/ml of penicillin and 100 mg/ml streptomycin (both obtained from Invitrogen S.A.). We also obtained pure neuronal cultures by growing cells in MEM supplemented with B27 (Invitrogen). Cell cultures were incubated at 37°C in a 5% CO_2 atmosphere. At 4 days in vitro for overexpression analyses and at 5 days in vitro for colocalization studies, cultures were fixed with 4% paraformaldehyde solution (PFA; Merck Biosciences Ltd., Nottingham, United Kingdom) in phosphate-buffered saline, pH 7.4 (PBS), and processed for immunocytochemistry.

Neurosphere assay

We used a neurosphere assay in vitro to study the role of Ikaros family members in embryonic NPCs. For neurosphere cultures, LGEs from E14.5 wt mice were dissected out and disaggregated mechanically with a fire-polished Pasteur pipette until no aggregates could be seen. Thereafter, 1.25×10^6 cells were plated at a density of 50,000 cells/cm^2 in complete medium [Dulbecco's modified Eagle's medium (DMEM; Sigma Chemical Co.):F12 (Invitrogen S.A.; 1:1); supplemented with 30% glucose, 1 M Hepes, 0.2% heparin, 4 mg/ml BSA, 1 × N2 supplement (Invitrogen S.A.), 0.3 mg/ml L-glutamine (Invitrogen S.A.), and 50 U/ml penicillin/streptomycin]. To allow neurosphere formation, complete medium was supplemented with 20 ng/ml fibroblast growth factor (FGF; Sigma Chemical Co) and 10 ng/ml epidermal growth factor (EGF; Invitrogen S.A.). After 5 days in vitro, we mechanically disaggregated the neurospheres to single cells and seeded them again for neurosphere formation at a density of 10,000 cells/cm^2. Low-passage neurospheres (between 4 and 6) were transfected as described below. Thereafter, viable cells were counted by trypan blue exclusion. For proliferation assays, 2 days after transfection, neurospheres from LGE were treated with 1 mM of BrdU for 20 minutes, fixed, and processed for immunohistochemistry.

To analyze NPCs derived from *Ikaros*$^{-/-}$ embryos, individual forebrains from E14.5 embryos from the different genotypes were dissected, disaggregated into small pieces, and digested enzymatically with trypsin 0.05% (Invitrogen S.A.) for 15 minutes at 37°C. Digestion was halted by the addition of culture medium [DMEM (Sigma Chemical Co.):F12 (Invitrogen S.A.; 1:1); supplemented with 1.5% glucose, 2 mM glutamine, 10 mM Hepes, 10% FBS, and 50 U/ml penicillin/streptomycin (Invitrogen S.A.)]. Thereafter, tissue samples were treated with 6.5 mg/ml DNAse (Sigma Chemical Co.) for 10 minutes at 37°C and centrifuged for 10 minutes at 1,000 rpm. Cells were cultured at 37°C in a 5% CO_2 atmosphere. Twenty-four hours later, each plate was expanded in serum-free medium [DMEM (Sigma Chemical Co.):F12 (Invitrogen S.A.; 1:1) supplemented with: 1.5% glucose, 2 mM glutamine, 1 M Hepes, 50 U/ml penicillin/streptomycin, 1× N2 supplement (Invitrogen S.A.), 4 ng/ml EGF, 25 ng/ml FGF (both obtained from R&D Systems Inc., Minneapolis, MN), and 2 μg/ml heparin (Sigma Chemical Co.)]. Cells were grown in suspension for 5 days.

Cell transfection

To overexpress Ikaros-1, we transfected the cells with the pMX-IK1-IRES-GFP plasmid (Gomez-del-Arco et al., 2004) or the MSCV-Ik-1-IRES-GFP plasmid (Kathrein et al., 2005), which encode for the Ikaros-1 isoform and enhanced green fluorescent protein (eGFP). We used plasmids that express only eGFP, the pmax-eGFP plasmid (Amaxa Biosystems, Cologne, Germany), or the MSCV-IRES-GFP (Kathrein et al., 2005) as controls for Ikaros-1 overexpression.

Embryonic neurospheres were disaggregated mechanically and transfected by nucleofection, following the manufacturer's protocol (Amaxa Biosystems). Cells (5×10^6) were transfected with 12 μg of the given plasmid, using the A33 Nucleofector program (Amaxa Biosystems). The efficiency of transfection is between 40% and 50% of cells.

Primary cultures were transfected 24 hours after seeding with 0.5 μg of the plasmids per well (24-well plate). The transfection was done with Lipofectamine LTX (Invitrogen S.A), following the manufacturer's instructions, which results in an efficiency of transfection about 0.5–1% of cells. Three days after the transfection, cells were fixed with 4% PFA for immunocytochemistry analysis.

Antibody characterization

All immunostainings were performed using the antibodies listed in Table 2. Anti-BrdU antibody, clone Bu20a

TABLE 2.
Primary Antibodies Used for Immunocytochemistry, Immunohistochemistry, and Western Blot

Antigen	Manufacturer, catalog or lot No.	Species in which the antibody was made	Dilution	Immunogen used to generate antibody
Bromodeoxyuridine (BrdU)	Dako (Glostrup, Denmark) catalog M0744	Mouse	1:50	BrdU conjugated to bovine serum albumin
Bromodeoxyuridine (BrdU)	Megabase Research Products (Lincoln, NE) catalog BP41000	Rabbit	1:1,500	BrdU coupled to keyhole limpet hemocyanin (KLH)
Calbindin	Sigma Chemical Co. (St. Louis, MO) catalog C9848	Mouse	1:1,000	Purified bovine kidney calbindin-D28K
ChAT	Millipore (Billerica, MA) catalog AB143	Rabbit	1:4,000	Human placental enzyme
DARPP-32	Millipore catalog AB1656	Rabbit	1:500	Synthetic peptide (CQVEMIRRRRPTPAM) coupled to KLH
GFAP	Dako catalog Z0334	Rabbit	1:500	GFAP purified from bovine spinal cord
GFP-FITC	Abcam (Cambridge, United Kingdom) catalog ab6662	Goat	1:200	Full-length GFP (amino acid sequence 246 aa)
Ikaros	Katia Georgopoulos	Mouse	1:2,000	Peptide comprising aa 300-390
MAP2	Sigma Chemical Co. catalog M1406	Mouse	1:500	Bovine microtubule-associated protein 2
Nestin	Covance (Denver, PA) catalog PRB-315C	Rabbit	1:200	KLH-conjugated peptide (CPSQPLKFTLSGVDGDSWSSGED) to the mouse C-terminal nestin tail
NeuN	Millipore (Billerica, MA) catalog MAB377	Mouse	1:100	Purified cell nuclei from mouse brain
Cleaved Notch-1	Cell Signalling Technology (Danvers, MA) catalog 2421	Rabbit	1:100	Synthetic peptide (VLLSRKRRRQH) coupled to KLH
p21	Santa Cruz Biotechnology (Santa Cruz, CA) catalog sc-397	Rabbit	1:200	Peptide corresponding to aa 146-164 mapping at the C-terminus of human p21
p27 (Kip1)	BD Biosciences (Erembodegem, Belgium) catalog 610241	Mouse	1:500	Mouse Kip1 aa. 1-197
Parvalbumin	SWANT (Bellinzona, Switzerland) catalog PV-28	Rabbit	1:1,000	Rat muscle parvalbumin
βIII-Tubulin	Sigma Chemical Co. catalog T2200	Rabbit	1:200	Synthetic peptide corresponding to aa 441-450 of human βIII-tubulin

(Dako, Glostrup, Denmark), recognized BrdU incorporated into DNA in place of thymidine during DNA synthesis by immunocytochemistry (Magaud et al., 1989), flow cytometry (Dolbeare et al., 1983), or ELISA (Magaud et al., 1988). Similarly, anti-BrdU antibody (Megabase Research, Lincoln, NE) showed by ELISA a good signal binding to BrdUTP-substituted DNA. No cross-reactivity to 5-methyl cytosine or deoxiuridine was observed (manufacturer's data sheet). As a negative control, the antibody failed to stain embryonic mouse brains that were not injected with BrdU (Supp. Info. Fig. 2).

The calbindin D-28 antibody (Sigma Chemical Co.) recognized a single band of 28 kDa molecular weight (m.w.) on Western blots of rat brain (manufacturer's data sheet), and stained a pattern of cellular morphology and distribution in the mouse retina that is identical to that in previous reports (Haverkamp and Wassle, 2000). Within the striatum, this antibody recognizes striatal projecting neurons in a pattern that was identical to that in previous descriptions (Perez-Navarro et al., 1996).

The anticholine acetyltransferase (ChAT) polyclonal antibody (Millipore, Billerica, MA) precipitated a 68-kDa protein corresponding to ChAT as well as an unrelated 27-kDa protein from human motor neurons (manufacturer's technical information). In mouse brain, it stained a cytoplasmic pattern in interneurons in the cerebral cortex (Bhagwandin et al., 2006) and large neurons in the striatum (Canals et al., 2004; Bloomfield et al., 2007), which is consistent with previous reports.

The anti-DARPP-32 polyclonal antibody (Millipore) recognized a band of 32 kDa m.w. on Western blots of mouse brain (Torres-Peraza et al., 2007) and stained neurons in tissue sections in a pattern that was identical to that in previous descriptions (Canals et al., 2004) and in primary cultures by immunostaining (manufacturer's data sheet).

The anti-GFAP polyclonal antibody (Dako) recognized a single band of 50 kDa m.w. on Western blots of mouse brain (manufacturer's data sheet). In mouse brain, it stained a pattern consistent with fibrillary astrocytes, as demonstrated previously in rat brain (Yasuda et al., 2004). The staining pattern was also consistent with that of transgenic mice that express the LacZ under the GFAP promoter (Brenner et al., 1994).

Fluorescein conjugated anti-GFP polyclonal antibody (Abcam, Cambridge, United Kingdom) stained cells containing GFP-expressing inserts in prokaryotic (*Escherichia coli*) and eukaryotic (CHO) cells (manufacturer's data sheet). As a negative control, the antibody failed to stain brains from wt mice (Supp. Info. Fig. 3).

The anti-Ikaros antibody recognized all eight Ikaros isoforms in the 66–36-kDa range by Western blot of lymphocyte whole cell lysates (Sun et al., 1999) and stained NIH 3T3 fibroblast cells transfected with Ikaros-1 plasmid (Georgopoulos et al., 1994). As a negative control, the antibody failed to stain brain tissue from Ikaros$^{-/-}$ mice (Supp. Info. Fig. 4).

The anti-MAP-2 monoclonal antibody (Sigma Chemical Co.) recognized a single band of 220 kDa m.w. on Western blots of rat brain (manufacturer's data sheet) and stained neurons in tissue sections or primary cultures (Binder et al., 1986).

The anti-nestin polyclonal antibody (Covance, Denver, PA) recognized a band of 220–240 kDa m.w. on Western blots of mouse embryonic cells and stained specifically filaments in Ntera-2 and mouse embryonic (Pallante et al., 2007) or neural (Bosch et al., 2004) stem cells as well as neonatal mouse brain sections (manufacturer's data sheet).

The anti-NeuN monoclonal antibody (Millipore) recognized two or three bands in the 46–48 kDa m.w. range and possibly another band at approximately 66 kDa m.w. (manufacturer's data sheet). It also stained neurons in primary cultures or brain tissue sections in a pattern that was identical to that in previous descriptions (Canals et al., 2001; Bosch et al., 2004).

The cleaved Notch1 polyclonal antibody (Cell Signalling Technology, Danvers, MA) recognized a single band of 110 kDa on Western blots of differentiated NIH/3T3 cells (manufacturer's data sheet) and stained COS cells transfected with human Notch 1 full-length cDNA and treated with EDTA (manufacturer's data sheet). Specific immunoreactivity has been observed on Western blot and immunostaining (Tokunaga et al., 2004).

Anti-P21 polyclonal antibody (Santa Cruz, Santa Cruz, CA) recognized a single band of 21 kDa m.w. on Western blots of C32 nuclear extracts (manufacturer's data sheet) or liver cells extracts (Jaime et al., 2002).

Anti-P27[Ki1] monoclonal antibody (BD Bioscience, Erembodegem, Belgium) recognized a single band of 27 kDa m.w. on Western blots of endothelial cells of porcine thoracic aortas and HeLa cells (Hirano et al., 2004) and stained HeLa cell nuclei (manufacturer's data sheet). We used this antibody only for Western blots and found protein expression levels consistent with mRNA expression levels.

The parvalbumin antiserum (Swant, Bellinzona, Switzerland) stained a pattern of neurons in the striatum and substantia nigra of mouse brain that was identical to that in previous descriptions (Perez-Navarro et al., 1996; Gratacos et al., 2001; Canudas et al., 2005). This antibody recognizes a single band of about 14 kDa m.w. on Western blot of mouse cerebellar samples that was not detected in knockout mice (Caillard et al., 2000).

Anti-βIII-tubulin antibody (Sigma Chemical Co.) recognized a single band of 55 kDa m.w. on Western blots of cultured cells or brain lysates. Additional weak bands may be detected when immunoblotting some extract preparations (manufacturer's data sheet). βIII-Tubulin antibody also stained neurons of the central and peripheral nervous systems in primary cultures or brain tissue sections (Bosch et al., 2004; Cleary et al., 2006).

Immunolabelling

Fluorescent immunolabelling was performed according to the protocol described by Bosch et al. (2004). In brief, cultures or tissue sections were fixed with 4% paraformaldehyde in 0.1 M phosphate buffer (pH 7.4) for 45 minutes. Cultures and/or tissue sections were blocked for 1 hour in PBS containing 0.3% Triton X-100 and 30% normal horse serum (NHS; Gibco-BRL). Thereafter, they were incubated overnight at 4°C in PBS containing 0.3% Triton X-100 and 5% NHS with the corresponding primary antibodies. After three PBS washes, cultures were incubated for 2 hours at room temperature with the following secondary antibodies: FITC-conjugated anti-rabbit (1:100; Vector Laboratories, Burlingame, CA), Cy3-conjugated donkey anti-rabbit IgG (1:500), Cy2-conjugated donkey anti-mouse (1:200), and Texas red-conjugated donkey anti-mouse (1:200; all from Jackson Immunoresearch Laboratories Inc., West Grove, PA). Cultures or tissue sections were counterstained with 4′,6-diamidino-2-phenylindole, dihydrochloride (DAPI; Sigma Chemical Co.) and mounted in Mowiol (Calbiochem, La Jolla, CA). Fluorescent photomicrographs were taken on a Leica TCS SL laser scanning confocal spectral microscope (Leica Microsystems Heidelberg GmbH, Manheim, Germany). All pictures acquisitions were as tiff files, and adjustments of brightness and contrast were made in Adobe Photoshop 6.0.

To analyze the cellular populations of the striatum, mice were transcardially perfused with 4% paraformaldehyde in 0.1 M phosphate buffer (pH 7.4). Brains were removed,

TABLE 3.
Nucleotide Sequences of In Situ Hybridization Probes

Plasmid name	Source	Type of probe	Insert size (bp)	cDNA nucleotides of probe or nucleotides from 3′-end
Dlx2	John Rubenstein	Riboprobe	1,700	1,700 from 3′-end
Dlx5	John Rubenstein	Riboprobe	1,600	1,600 from 3′-end
Ebf1	Rudolf Grosschedl	Riboprobe	737	193-930
ENK	OPERON	Oligonucleotide	47	388-435
Ikaros	OPERON	Oligonucleotide	44	93-137
Ikaros	Katia Georgopoulos	Riboprobe	1,093	243-1,336
SP	OPERON	Oligonucleotide	47	145-192

postfixed for 2 hours at 4°C in the same solution, cryoprotected in PBS containing 30% sucrose, and frozen in dry ice-cooled isopentane. Serial coronal cryostat sections (30 μm thick) through the whole striatum were collected as free-floating sections in PBS and processed for immunohistochemistry as previously described (Canals et al., 2004). In brief, sections were incubated for 30 minutes with PBS containing 10% methanol and 3% H_2O_2 in order to block endogenous peroxidases. Sections were then washed three times in PBS and blocked for 1 hour with 2–10% normal serum in PBS. Tissue was then incubated with the appropriate primary antibody in PBS containing 2% normal goat serum for 16 hours at 4°C, except for DARPP-32, which was incubated at room temperature. Sections were washed three times and incubated with a biotinylated secondary antibody (1/220; Pierce, Rockford, IL) for 1–2 hours at room temperature in the same buffer as the primary antibody. The immunohistochemical reaction was developed using the ABC kit (Pierce). No signal was detected in control preparations from which the primary antibody was omitted.

In situ hybridization

For in situ hybridization, brains were removed at specific developmental stages and frozen in dry-ice-cooled isopentane. Serial coronal cryostat sections (14 μm) were cut on a cryostat, collected on silane-coated slides, and frozen at −20°C. Table 3 lists the genes and the nucleotide positions used for the probes in the in situ analysis.

Radioactive in situ hybridization was performed as described elsewhere (Perez-Navarro et al., 1999), using the following oligonucleotide probes: Ikaros, complementary to nucleotides 93–137 of the Ikaros sequence (GenBank accession No. NM_009578); ENK, complementary to nucleotides 388–435 of rat preproenkephalin (GenBank accession No. NM_001002927); and SP, complementary to nucleotides 145–192 of rat preprotachykinin A (GeneBank accession No. NM_009311). Oligoprobes were synthesized by OPERON (Qiagen GmbH, Hilden, Germany). In brief, sections were serially thawed and fixed with 4% paraformaldehyde in PBS, dehydrated in graded ethanol solutions and chloroform, and air dried. Oligonucleotide probes were 3′-end-labelled with α[^{35}S]dATP (GE Healthcare España S.A., Barcelona, Spain) using terminal deoxyribonucleotidyltransferase (Promega, Madison, WI). Labelled probes were separated from unincorporated nucleotides on a Nensorb-20 column (Du Pont, Wilmington, DE). The sections were hybridized at 42°C for 16 hours in a humidified chamber with 150 μl of hybridization cocktail [50% formaminde, 4× SSC (1× SSC: 0.15 M sodium chloride-0.015 sodium citrate buffer, pH 7.0), 1× Denhardt's solution, 10% dextran sulfate, 0.25 mg/ml yeast tRNA, 0.5 mg/ml sheared salmon sperm DNA, 1% sarcosyl (*N*-lauroy sarcoside), 0.02 M Na_3PO_4 (pH 7.0), 0.05 M dithiotreitol] per slide containing 5×10^6 c.p.m./ml of the probe. After hybridization, sections were rinsed and washed five times for 20 minutes in 0.1× SSC at 40°C, dehydrated in ethanol, and air dried. Then, the slides were exposed to β-max X-ray film (GE Healthcare España S.A.) for 20 days and dipped in LM-1 photoemulsion (GE Healthcare España S.A.) for 40 days at 4°C, developed in D-19 (Eastman Kodak Company, Rochester, NY), fixed, and counterstained with cresyl violet before analysis. Addition of 100-fold excess of unlabelled probe abolished all hybridization signals showing the specificity of the hybridization.

Nonisotopic in situ hybridization was performed as described elsewhere (Schaeren-Wiemers and Gerfin-Moser, 1993; Georgopoulos et al., 1994; Serrats et al., 2003; Flames et al., 2004), using riboprobes for Ikaros (Georgopoulos et al., 1994), Ebf-1 (Garel et al., 1999), or Dlx-2 or Dlx-5 (Flames et al., 2004) and oligoprobes for ENK and SP (Canals et al., 2004). In brief, frozen tissue sections were air dried, fixed in 4% paraformaldehyde in PBS for 20 minutes at 4°C, washed once in 3× PBS and twice in 1× PBS for 5 minutes each, and incubated for 2 minutes at 21°C in a freshly prepared solution of predigested Pronase (Calbiochem) at a final concentration of 24 U/ml in 50 mM Tris-HCl, pH 7.5, 5 mM EDTA. Enzyme activity was stopped by immersion for 30 seconds in 2 mg/ml glycine in PBS. Tissue sections were finally rinsed in PBS and dehydrated through a graded series of ethanol. Tissue sections were then covered with 100 μl of hybridization buffer containing the probes, overlaid with Nescofilm coverslips (Bando

Chemical, Kobe, Japan), and incubated overnight in humidified boxes at 42°C. Digoxigenin (DIG)-labeled probes were diluted in hybridization solution [50% formamide, 4× SSC (1× SSC: 150 mM NaCl, 15 mM sodium citrate), 1× Denhardt's solution, 10% dextran sulfate, 1% Sarkosyl, 20 mM phosphate buffer, pH 7.0, 250 μg/ml yeast tRNA, and 500 μg/ml salmon sperm DNA] to a final concentration of 1.5 nM. The oligodeoxyribonucleotide probes were 3′-end-labeled with terminal deoxynucleotidyltransferase and DIG-11-dUTP (Roche). DIG-labeled oligonucleotides were purified by ethanol precipitation and resuspended in 200 μl TE (10 mM Tris-HCl, pH 7.5, 1 mM EDTA, pH 8.0). After hybridization, sections were washed four times (45 minutes each) in a buffer containing 0.6 M NaCl and 10 mM Tris-HCl, pH 7.5, at 60°C. To develop the hybridization signal, the slides were immersed for 30 minutes in a buffer containing 0.1 M Tris-HCl, pH 7.5, 1 M NaCl, 2 mM $MgCl_2$, and 0.5% bovine serum albumin and incubated overnight at 4°C in the same solution with alkaline phosphate-conjugated antidigoxigenin-F(ab) fragments (1:5,000; Roche). They were then washed three times in the same buffer and twice in an alkaline buffer (0.1 M Tris-HCl, pH 9.5, 0.1 M NaCl, and 5 mM $MgCl_2$). Alkaline phosphatase activity was developed by incubating the sections with 3.3 mg nitroblue tetrazolium and 1.65 mg bromochloroindolyl phosphate (Invitrogen S.A.) dissolved in 10 ml alkaline buffer. The enzymatic reaction was stopped by extensive rinsing in alkaline buffer with the addition of 1 mM EDTA. The sections were then dehydrated and air dried.

Quantitative (Q)-PCR assays

Gene expression was evaluated by Q-PCR assays, as previously described (Martin-Ibanez et al., 2007), using the following TaqMan Gene Expression Assays (Applied Biosystems, Foster City, CA): 18s, Hs99999901_s1; βIII-tubulin, Mm00727586_s1; nestin, Mm00450205_m1; Notch1, Mm00435245_m1; Notch3, Mm00435270_m1, Hes-1, Mm00468601_m1; Hes-5, Mm01266490_g1; RBPJK, Mm00770450_m1; Deltex, Mm00492297_m1; delta, Mm-00432841_m1; Jagged, Mm00496902_m1; Mash-1, Mm01228155_g1; P21, Mm00432448_m1; and P27, Mm00438168_m1. All Q-PCR assays were performed in duplicate and repeated in at least three independent experiments.

The Q-PCR data were analyzed and quantified using the comparative quantitation analysis program of MxPro Q-PCR analysis software version 3.0 (Stratagene, La Jolla, CA), with 18S gene expression as an internal loading control. For developmental studies, the results are expressed as relative levels of the expression in relation to E14.5 expression levels, considered as 1. For Ikaros-1 overexpression, the results are expressed as relative levels with respect to the control eGFP overexpression, considered as 100%.

Western blot

We analyzed which Ikaros isoforms were present in E18.5 and P15 striatum. Samples (n = 3) were prepared and processed for Western blot as described elsewhere (Canals et al., 2004). Thirty micrograms of striatal homogenates were loaded in a 7.5% SDS-PAGE (sodium dodecyl sulfate-polyacrylamide gel electrophoresis) and transferred to Immobilon-P membranes (Milipore, Bedford, MA). Blots were incubated overnight at 4°C with 1:1,000 of anti-Ikaros antibody (Molnar and Georgopoulos, 1994), and, after several washes in Tris-buffered saline with 0.1% v/v Tween-20 (TBS-T), membranes were incubated with an HRP-conjugated anti-mouse IgG (1:1,000; Promega) and developed by the ECL Western blotting system (Amersham Bioscience Europe GmbH, Freiburg, Germany).

To analyze the levels of $p21^{Cip1/Waf1}$, $p27^{Kip1}$, and cleaved Notch1 in Ikaros-transfected neurospheres, 20 μg of neurosphere homogenates in lysis buffer (0.2% SDS in 80 mM Tris-HCl, pH 6.8) was loaded in a 12% SDS-PAGE, transferred to Immobilon-P membranes, and incubated with the appropriate primary antibodies (see Table 2). Membrane signal was developed as described above.

In situ detection of cell death

Pregnant wt or *Ikaros*$^{-/-}$ mice were deeply anesthetized at E18.5, and fetal brains were then excised and frozen in dry ice-cooled isopentane. Cryostat-cut coronal sections (14 μm) were serially collected on silane-coated slides and processed to detect DNA fragmentation with the TdT-mediated dUTP nick-end labeling (TUNEL) technique, using the in situ Apoptosis Detection System (Promega), as described by Bosch et al. (2004). In brief, sections were immersed in cool ethanol/acetic acid (2:1 vol/vol) for 5 minutes and washed twice with PBS at room temperature. Sections were treated for 10 minutes with proteinase K (20 μg/ml) and postfixed in 4% paraformaldehyde in PBS for 5 minutes. Next, tissue sections were incubated with the equilibration buffer for 5 minutes at room temperature and then with fluorescein-12-dUTP and terminal deoxynucleotidyl transferase (TdT). After a 1-hour incubation at 37°C, sections were washed with 2× SSC for 15 minutes and three times with PBS for 10 minutes. As a negative control, adjacent sections were processed following the standard procedure, except that TdT was replaced by water. Finally, tissue sections were mounted with Mowiol (Calbiochem) and visualized by fluorescence microscopy.

Measurement of areas and cell counts

The volumes of certain brain regions were measured with ImageJ v1.33 by Wayne Rasband (National Institutes of Health, Bethesda, MD) on a computer attached to an Olympus microscope (Olympus Danmark A/S, Ballerup,

Denmark). Consecutive 30-μm-thick sections (14–16 sections/animal) were viewed, and the borders of the anatomical landmarks were outlined. The volume of the GZ was also measured as the proliferative area observed after BrdU administration. The volumes were calculated by multiplying the sum of all section areas (mm^2) by the distance between successive sections (0.3 mm), as described previously (Canals et al., 2004).

All cell counts were genotype-blind (n = 4–6 per each condition). Except for BrdU staining, we counted those cells showing a clear positive cytoplasm surrounding a less well-stained nucleus. Unbiased stereological counts were performed by using the Computer Assisted Stereology Toolbox (CAST) software (Olympus Danmark A/S). The number of positive cells in the striatum was estimated by using the optical dissector method (Gundersen et al., 1988). A grid size was chosen so that we counted a 10% of total striatal area. The unbiased counting frame was positioned randomly on the outline of the striatum by the software, thereby creating a systematic random sample of the area. Sections were viewed under a ×100 objective, and the counting field corresponded to 1,529.00 μm^2. Gundersen coefficients of error for m = 1 were all less than 0.10. For striatal cell counts, sections spaced 300 μm apart were analyzed as previously described (Canals et al., 2004). To count the number of BrdU-positive cells, we analyzed serial sections separated every 70 μm.

To determine the effect of Ikaros on the proliferation of NPCs in vitro, we counted the cells that incorporate BrdU per neurosphere after transfection with Ikaros-1 or eGFP and expressed the number counted as a percentage of the total number of cells per neurosphere identified by DAPI-counterstained nuclei (n = 3–5). At least 50 neurospheres were counted per transfection (the number of cells per neurospheres is between 20 and 50). Results were standardized in relation to control pmax-eGFP-transfected NPCs (considered as 100%).

To calculate the proliferation rate of fetal primary neurospheres formed from wt, heterozygous, or *Ikaros*$^{-/-}$ embryos, we counted the number of neurospheres by phase contrast at 5 days of neurosphere formation, and then, after disaggregating them, we counted the cells in a Neubauer chamber. Results are expressed as the percentage of each genotype in relation to wt mice (considered as 100%) from at least three independent experiments.

To determine the effect of Ikaros on the differentiation of LGE primary cultures, we counted the number of cells per coverslip overexpressing Ikaros-1 or GFP that colocalized with different markers, such as nestin, βIII-tubulin, calbindin, and enkephalin 3 days after the transfection. The results are expressed as the percentage of transfected cells colocalizing with the different markers with respect to the total number of transfected cells. Between 50 and 200 transfected cells per coverslip were counted per transfection (n = 3–5).

Statistical analyses

All results are expressed as the mean of independent experiments ± SEM. Results were analyzed by Student's *t*-test or one-way ANOVA, followed by the Bonferroni post hoc test.

RESULTS

Ikaros-1 is selectively expressed by immature neurons in the SVZ-MZ boundary

In agreement with the study of Agoston et al. (2007), we found that Ikaros expression was mostly restricted to the MZ of the LGE between E14.5 and P3, with a peak at about E18.5 (Supp. Info. Fig. 5a–h,j–l). We also observed that this expression showed a dorsomedial-to-ventrolateral gradient, with most of the Ikaros-expressing cells located at the GZ/MZ boundary (Supp. Info. Fig. 5b–e,l). Differential splicing of Ikaros gene generates up to eight different protein isoforms that can be detected by Western blot (Molnar et al., 1996; Rebollo and Schmitt, 2003). Our blot analysis demonstrated that Ikaros-1 was the most abundant isoform in the developing striatum at E18.5 (Supp. Info. Fig. 5i). Moreover, consistently with morphological results (Supp. Info. Fig. 5a–h,j–l), high levels of Ikaros-1 were detected at E18.5, but they had disappeared by P15 (Supp. Info. Fig. 5i). We also detected other isoforms of Ikaros that could be attributed to differentiating endothelial cells (Agoston et al., 2007).

To determine which cell types expressed Ikaros, we performed colocalization studies in primary cultures obtained from E14.5 mouse LGEs. Double immunocytochemistry showed that Ikaros was not expressed by nestin-positive NPCs (Fig. 1a–d) or by GFAP-positive astrocytes (Fig. 1e–h). However, Ikaros-positive cells colocalized mostly with βIII-tubulin (Fig. 1i–l). Consistently, the temporal pattern of Ikaros expression during LGE development correlated with the final period of nestin expression and with the expression profile of βIII-tubulin (Fig. 1m,n). In addition, double immunohistochemistry for BrdU and Ikaros performed in E14.5 embryos injected with a short pulse of BrdU showed that this transcription factor is expressed by postmitotic cells in the MZ but not in the proliferative GZ (Supp. Info. Fig. 6a–c). The fact that Ikaros is expressed by postmitotic immature neurons and located at the boundary between the GZ and the MZ led us to hypothesize that this transcription factor is involved in the striatal neurogenesis of NPCs that exit the GZ and enter the MZ.

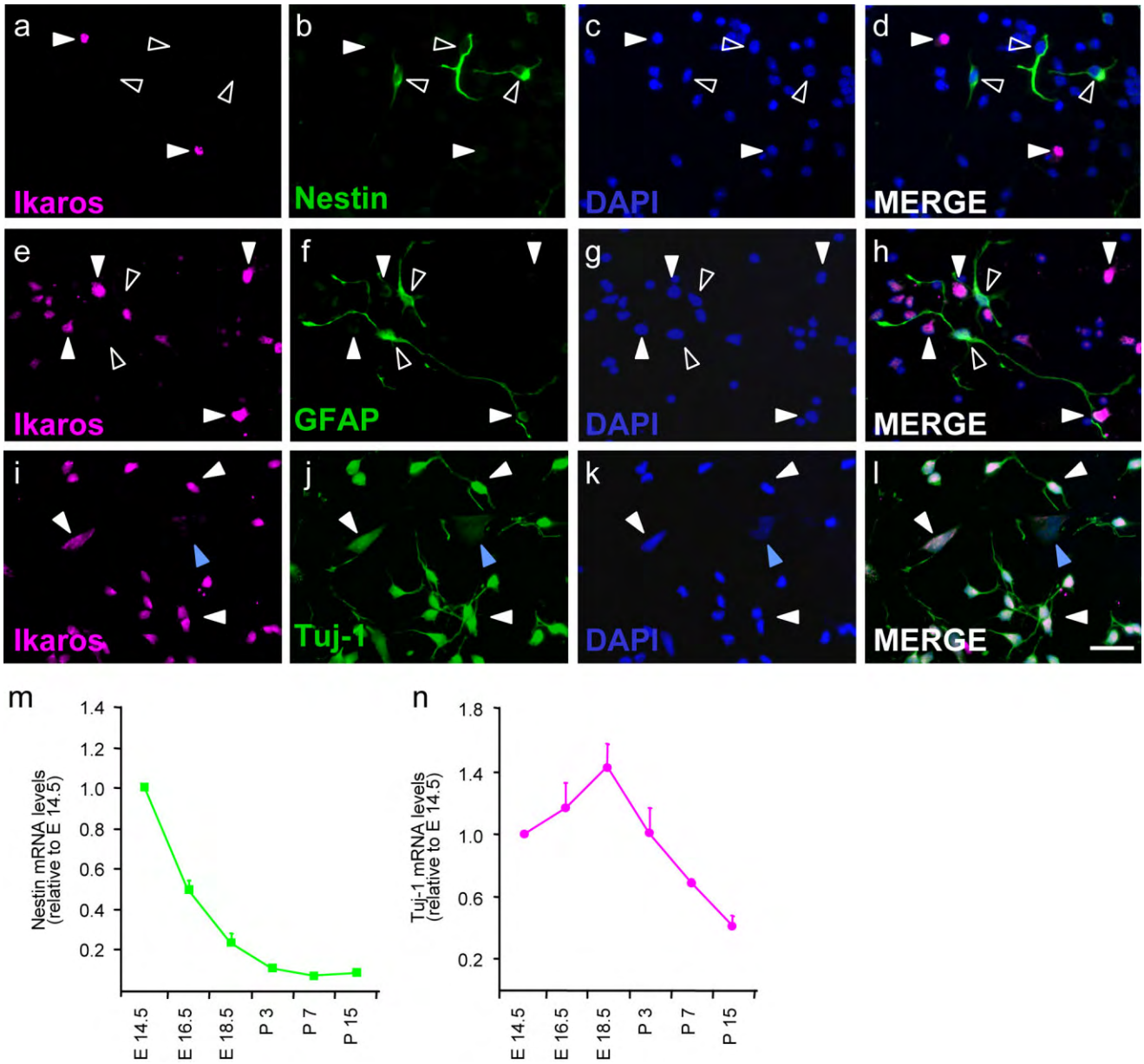

Figure 1. Ikaros is expressed by early postmitotic neurons in primary cultures from the LGE. **a–l:** Double-fluorescence immunocytochemistry performed on 5-day primary E14.5 LGE cultures. No Ikaros-expressing cells colocalize with the neural precursor marker nestin (a–d) or the astroglial marker GFAP (e–h). In addition, Ikaros-1 is located in cells that express the early neuronal marker βIII-tubulin (Tuj-1; i–l). a–l: Solid arrowheads show Ikaros-positive cells. a–h: Open arrowheads show single-stained cells for nestin or GFAP. i–l: Blue arrowheads show double-negative cells. **m,n:** Striatal samples at different stages of development (from E14.5 to P15) were analyzed by Q-PCR to study the patterns of expression of nestin (m) and βIII-tubulin (Tuj-1; n). The results are expressed as the mean of the levels of expression of each marker at each developmental stage studied in relation to the expression at E14.5, considered as 1, from at least three independent samples. Error bars represents the SEM. Scale bar = 30 μm.

Ikaros-1 induces neurogenesis throughout the regulation of p21$^{Cip1/Waf1}$

Overexpression of Ikaros-1 in neurospheres derived from E14.5 LGEs reduced the proliferation of NPCs from the level of the eGFP-transfected controls (Fig. 2a). Consistently, NPCs that overexpressed Ikaros-1 were negative for BrdU labeling (Fig. 2g–j). The effect of Ikaros on NPC proliferation was also confirmed by the characterization of primary neurospheres derived from *Ikaros*$^{-/-}$, heterozygous, and wt embryonic forebrains (Fig. 2b). The number of NPCs per neurosphere was greater in Ikaros-deficient samples than in wt-derived samples (Fig. 2b), indicating increased proliferation. In addition, NPCs overexpressing Ikaros-1 were differentiated toward immature βIII-tubulin-positive neurons (Fig. 2p–t), whereas

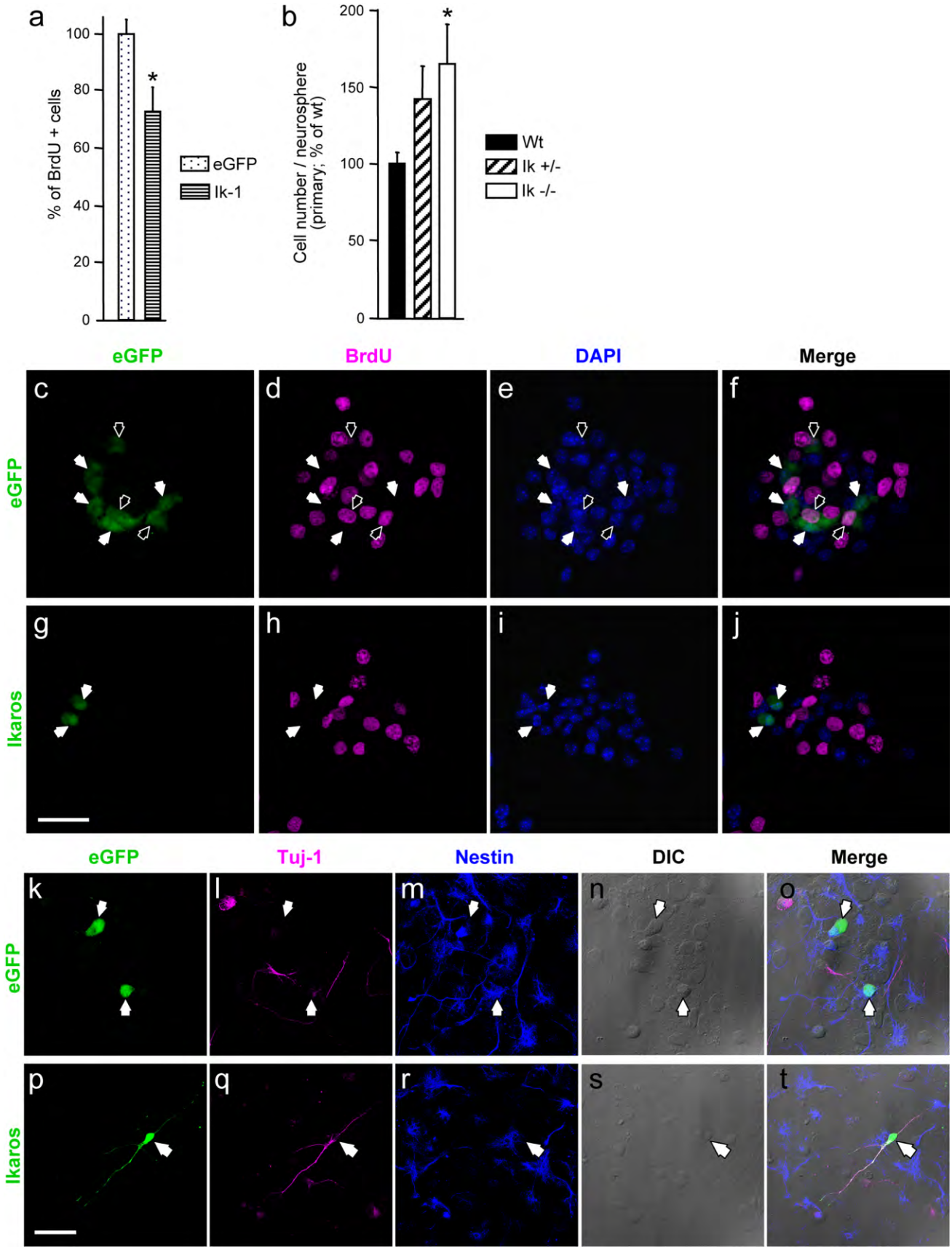
a
% of BrdU + cells
100
80
60
40
20
0
*
eGFP
Ik-1
b
Cell number / neurosphere (primary; % of wt)
200
150
100
50
0
*
Wt
Ik +/-
Ik -/-
eGFP
BrdU
DAPI
Merge
c
d
e
f
eGFP
g
h
i
j
Ikaros
eGFP
Tuj-1
Nestin
DIC
Merge
k
l
m
n
o
eGFP
p
q
r
s
t
Ikaros

Figure 2

NPCs overexpressing eGFP mainly colocalized with nestin-positive cells (Fig. 2k–o). Similar results were obtained when primary cultures obtained from E14.5 LGEs were transfected with Ikaros-1 and analyzed 3 days later (Fig. 3). Ikaros-1-overexpressing cells barely colocalized with the neural precursor marker nestin, compared with the control eGFP-overexpressing cells (Fig. 3a–m; nestin-positive cells/transfected cells; Ikaros-1 (Ik-1): 6.11% ± 3.18%, eGFP: 44.13% ± 6.49%; 86.3% of reduction). Interestingly, Ikaros-1-overexpressing cells showed a 56% increase of colocalization with the neuronal marker βIII-tubulin over control eGFP-transfected cells (Fig. 3a–l,n; β-tubulin III-positive cells/transfected cells; Ikaros-1 (Ik-1): 80.32% ± 3.52%, eGFP: 51.40% ± 2.04%).

Within the hematopoietic system, Ikaros controls proliferation through the regulation of the levels of cyclin-dependent kinase inhibitors (CDKi), such as $p27^{Kip1}$ (Kathrein et al., 2005). Thus, we analyzed whether CDKi participates in Ikaros-1-induced neurogenesis (Fig. 4). Western blot analysis showed that Ikaros-1-overexpressing neurospheres presented higher levels of expression of $p21^{Cip1/Waf1}$ than did controls transfected with eGFP (Fig. 4a; Ikaros-1: 130.7% ± 0.21% of increase over eGFP controls). However, the levels of $p27^{Kip1}$ under these two conditions did not differ (Fig. 4a; Ikaros-1: 115% ± 16.5% increase over eGFP controls). We also analyzed the mRNA levels of $p21^{Cip1/Waf1}$ and $p27^{Kip1}$. Consistently, Q-PCR showed an increase of $p21^{Cip1/Waf1}$ mRNA levels (Fig. 4b; 156.8% ± 28.33% of increase over eGFP controls), whereas the expression of $p27^{Kip1}$ did not change (Fig. 4b; 85.2% ± 11.52% of increase over eGFP controls). To analyze this effect further, we studied the effect of Ikaros-1 overexpression on the proliferation of neurospheres obtained from *p21*$^{-/-}$ mice (Fig. 4c). Although Ikaros-1 overexpression reduced BrdU incorporation in neurospheres obtained from wt mice, this effect was completely absent in neurospheres from *p21*$^{-/-}$ mice (Fig. 4c). We also studied the possible involvement of Notch pathway in Ikaros-1-mediated neurogenesis of NPCs. Quantitative Q-PCR analyses of the levels of expression of different Notch pathway-related proteins showed no differences between neurospheres overexpressing Ikaros-1 or eGFP (Fig. 4d). Consistently, the levels of Notch1 intracellular domain in protein extracts derived from neurospheres overexpressing Ikaros-1 or eGFP were not significantly different (Fig. 4e).

Figure 2. Ikaros-1 induces neurogenesis in neurosphere cultures from the LGE. Neurospheres obtained from E14.5 LGE were used to study the effect of Ikaros-1 on the proliferation of embryonic NPCs. **a:** Overexpression of Ikaros-1 (Ik-1) in embryonic NPCs led to fewer cells incorporating BrdU than in control NPCs transfected with the eGFP plasmid (n = 3–5). Results are expressed as the percentage of BrdU-positive cells per neurosphere, standardized to those obtained from eGFP, considered 100%. **b:** Proliferation rate of NPCs obtained from E14.5 wt, heterozygous (Ik +/–), or Ikaros$^{-/-}$ (Ik –/–) mouse forebrains (n = 3–5). Graphs show the number of cells per primary neurosphere. Results are standardized to those obtained from wt mice, considered as 100%. **c–j:** Representative photomicrographs showing the lack of colocalization between Ikaros-1 and BrdU, whereas controls overexpressing eGFP alone colocalize with both BrdU-positive and -negative cells. Open arrows show double-stained cells for eGFP and BrdU. **k–t:** Ikaros-1 induces neuronal differentiation of NPCs. Representative photomicrographs of distinct NPCs, showing triple immunocytochemistry for eGFP and the neural and neuronal markers nestin and βIII-tubulin (Tuj-1). Note that Ikaros-1-overexpressing cells colocalize with βIII-tubulin-positive immature neurons, whereas control eGFP-transfected cells mainly colocalize with nestin-positive neural precursors. Arrows show eGFP-Ikaros positive cells. a,b: Results are expressed as the mean of three to five transfections (a) or mice (b). Error bars represent the SEM. Statistical analysis was performed with the Student's *t*-test. $^*P < 0.05$ relative to eGFP-transfected NSCs (a) or wt neurospheres (b). Scale bars = 50 μm.

Ikaros is a critical factor for the correct development of late-born ENK-positive striatal projecting neurons

To confirm the results obtained in vitro, we next characterized the striatal neurogenesis in *Ikaros*$^{-/-}$ embryos. To this end, we first analyzed the relative volumes of the striatum, the GZ, and the olfactory bulb at E18.5 (Fig. 5), because *Ikaros*$^{-/-}$ embryos had smaller brains than wt ones at E18.5 (26.9% reduction). There was less MZ in *Ikaros*$^{-/-}$ embryos at E18.5 than in wt mice (Fig. 5a,e,f). This reduction was accompanied by an increased volume of the GZ (Fig. 5b,d–f). However, there were no differences in the relative volume of the olfactory bulb (Fig. 5c), another structure derived from the LGE (Alvarez-Buylla et al., 2002; Stenman et al., 2003). Enlarged proliferating GZ in *Ikaros*$^{-/-}$ mice could be a consequence of the incapacity of NPCs to differentiate into MZ neurons. For this reason, we performed a series of birth-dating experiments in *Ikaros*$^{-/-}$ embryos, as described in Materials and Methods (Supp. Info. Fig. 1). No significant differences between wt and *Ikaros*$^{-/-}$ embryos were found in the density of BrdU-positive cells in the GZ or the MZ of mice injected at E12.5 (Fig. 6a), when early-born neurons are generated (Mason et al., 2005). However, *Ikaros*$^{-/-}$ embryos had a lower density of neurons exiting the cell cycle at E14.5 (Fig. 6b), a time coinciding with the generation of late-born striatal neurons (Mason et al., 2005). No differences between genotypes were detected in mice injected at E16.5 (Fig. 6c). Thus, lack of Ikaros blocks the generation of early stages of matrix striatal neurons. Consistently with these findings, we observed that Ikaros was expressed by late-born matrix neurons, insofar as there was a complementary pattern of expression between Ikaros and DARPP-32, a patch-

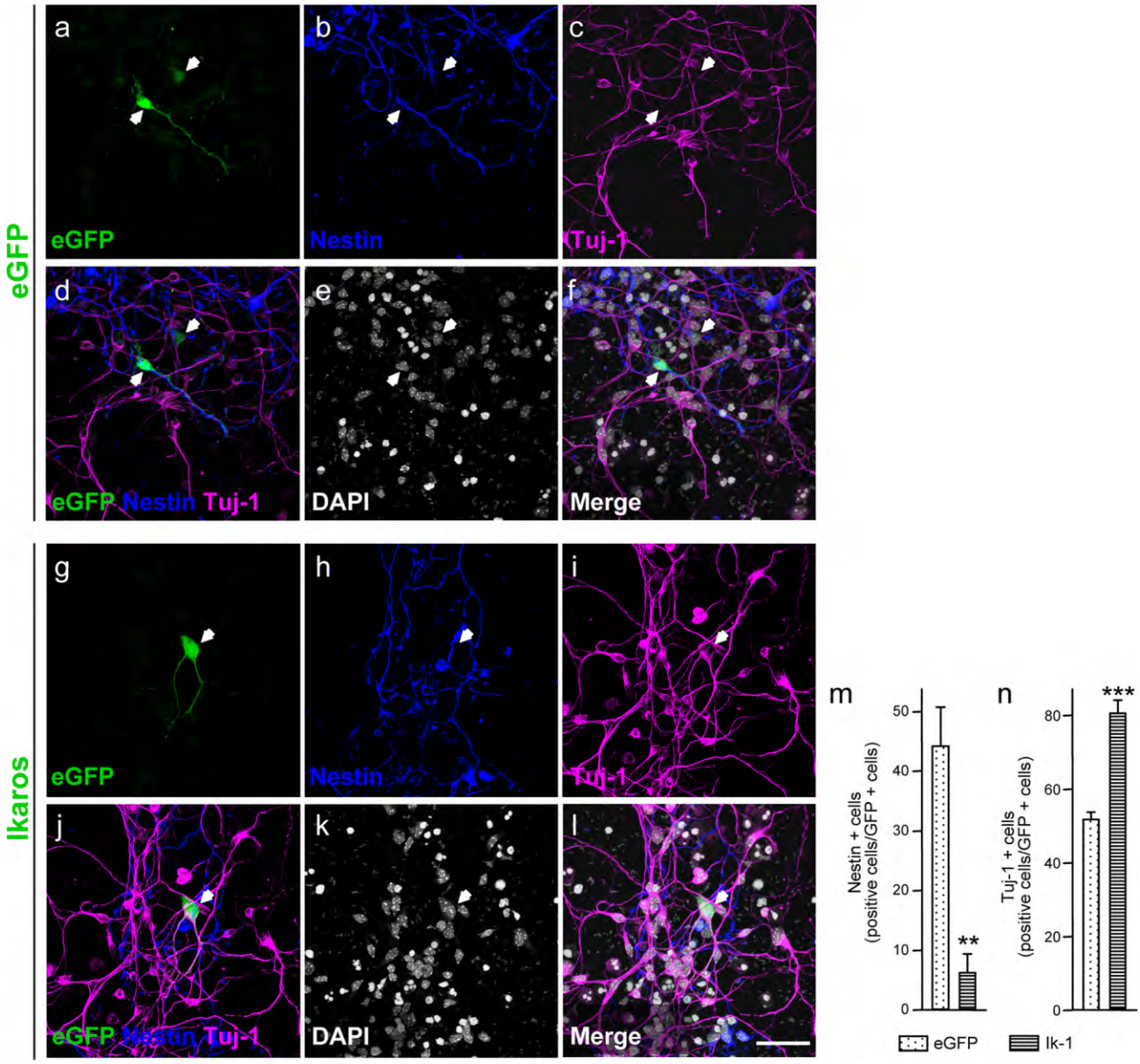

Figure 3. Ikaros-1 induces neuronal differentiation of striatal primary cultures. Colocalization studies performed in primary cultures obtained from LGE at E14.5 overexpressing Ikaros-1 or eGFP alone as a control for 3 days. **a–l:** Representative photomicrographs showing triple immunocytochemistry for eGFP, nestin, and βIII-tubulin (Tuj-1) in primary cultures overexpressing Ikaros-1 or eGFP alone. Arrows show eGFP-positive cells. **m,n:** Quantification of the number of Ikaros-1- and eGFP-positive cells colocalizing with nestin (m) and βIII-tubulin (Tuj-1; n). Graph bars represent the percentage of transfected cells positive for each marker out of the total number of transfected eGFP-positive cells. Ikaros-1-overexpressing cells become βIII-tubulin-positive immature neurons, whereas control cells overexpressing eGFP colocalize with both nestin- and Tuj-1-positive cells. Results are expressed as the mean of three to five transfected LGE primary cultures and error bars represent the SEM. Statistical analysis was by Student's *t*-test. $^{**}P < 0.005$, $^{***}P < 0.001$ relative to eGFP-transfected primary cultures. Scale bar = 50 μm.

compartment marker during development (Supp. Info. Fig. 7).

The reduction in BrdU-positive cells in the MZ of *Ikaros*$^{-/-}$ embryos could result not only from impaired proliferation but also from excessive cell death. GZ proliferation was studied in E14.5 embryos obtained from dams that had been injected with BrdU 30 minutes before. The density of proliferating cells in the GZ of *Ikaros*$^{-/-}$ embryos was higher than in wt ones (Fig. 6d–f). However, there were no differences in the levels of cell death between wt and *Ikaros*$^{-/-}$ embryos (Fig. 6g,h), indicating that naturally occurring cell death was not affected by the lack of this transcription factor. Taken together, these results suggest that lack of Ikaros compromises the second wave of stria-

tal neurogenesis, which in turn increases NPC proliferation at GZ. NPCs accumulated in the GZ of *Ikaros*$^{-/-}$ embryos could finally differentiate into glial cells, in that we observed an increase of GFAP-positive cells in adult *Ikaros*$^{-/-}$ mice with respect to wt mice (Fig. 6i–j).

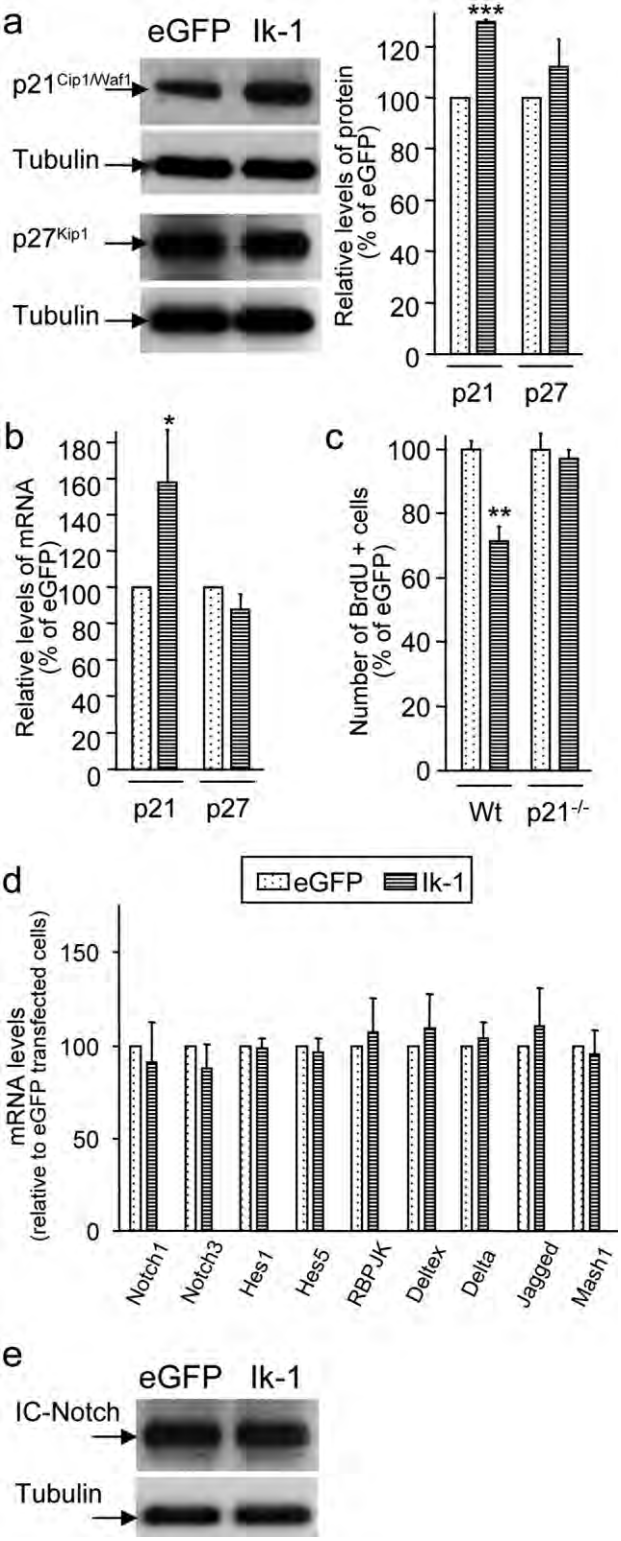

We next characterized the striatal volume and neuronal populations of adult wt and *Ikaros*$^{-/-}$ mice by accurate, nonbiased stereological analysis. In *Ikaros*$^{-/-}$ mice, there was a slight reduction in total brain volume (18.85%; Fig. 7a–c), which could be associated with a deficit of growth hormone secretion in these mice (Ezzat et al., 2006). Interestingly, striatal volume was severely affected in adult *Ikaros*$^{-/-}$ mice (35.24%; Fig. 7a–c). To test the affection of striatal projection neurons, we counted the number of calbindin- and DARPP-32-positive striatal cells. *Ikaros*$^{-/-}$ mice had a significantly lower density of calbindin-positive neurons than did wt mice (29.25% less; Fig. 7d). Similarly, *Ikaros*$^{-/-}$ mice also showed a lower density of DARPP-32-positive neurons than wt mice (26.8% less; Fig. 7e–g). Because two subpopulations of striatal projection neurons are defined on the basis of SP and ENK expression (Gerfen, 1992), we next analyzed them in *Ikaros*$^{-/-}$ mice. In situ hybridization studies showed that *Ikaros*$^{-/-}$ mice had lower relative levels of ENK expression than wt, but no differences in SP expression (28% of ENK reduction; Supp. Info. Fig. 8). This decrease in ENK levels of expression was due to a reduction in the number of ENK-positive neurons, insofar as their density was lower in Ikaros$^{-/-}$ mice than in wt mice (Fig. 7h). However, no differences in the expression levels or in the density of SP-positive neurons were detected (Fig. 7i; Supp. Info. Fig. 8). Finally, to test the specific affection of striatal projection neurons, we analyzed the number of striatal interneurons. No differences were found between *Ikaros*$^{-/-}$ and wt mice in the density of GABAergic

Figure 4. p21$^{Cip1/Waf1}$ is essential for Ikaros-1-regulated cell cycle arrest. Neurospheres obtained from E14.5 LGE were used to study the mechanism by which Ikaros-1 regulates the proliferation of embryonic NPCs. **a:** Western blot showing the levels of expression of p21$^{Cip1/Waf1}$ and p27^{Kip1} in neurospheres overexpressing Ikaros-1 (Ik-1) and the control eGFP. Graphs show the relative levels of p21$^{Cip1/Waf1}$ and p27^{Kip1}, indicating an increase of expression of p21$^{Cip1/Waf1}$ with respect to the control eGFP in NPCs. Results are expressed as the levels of p21$^{Cip1/Waf1}$ and p27^{Kip1} in relation to the control eGFP, considered as 100%. **b:** Q-PCR shows increased levels of mRNA of p21$^{Cip1/Waf1}$, but not of p27^{Kip1}, in neurospheres overexpressing Ikaros-1 (Ik-1). **c:** Ikaros-1 (Ik-1) overexpression in neurospheres derived from E14.5 LGEs of wt or *p21*$^{-/-}$ mice. Graphs show that Ikaros-1 decreases the incorporation of BrdU in wt- but not in *p21*$^{-/-}$-derived neurospheres. Results are expressed as the percentage of BrdU-positive cells in the culture in relation to the control eGFP, considered as 100%. **d:** mRNA levels of expression of different proteins involved in the Notch signaling pathway measured in neurospheres overexpressing Ikaros-1 (Ik-1) or eGFP ($n = 3–5$) by Q-PCR. **e:** Representative Western blot showing the lack of differences between the levels of expression of Notch1 intracellular domain in neurospheres overexpressing Ikaros-1 (Ik-1) and the control eGFP. a–d: Results are expressed as the mean of three to five transfections, and error bars represent the SEM. Statistical analysis was by Student's *t*-test. $*P < 0.05$, $**P < 0.005$, $***P < 0.001$ relative to eGFP-transfected NPCs.

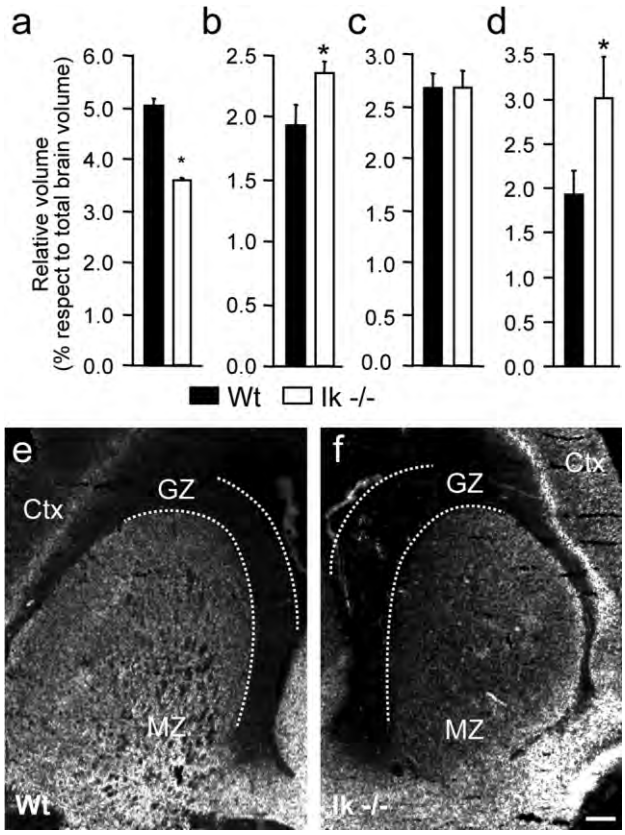

Figure 5. *Ikaros*$^{-/-}$ mice show reduced striatal volume but enlarged SVZ. **a–c:** Relative volumes of mantle zone (MZ; a), germinal zone (GZ; b), and olfactory bulb (OB; c) examined by anatomical landmarks in wt and *Ikaros*$^{-/-}$ embryos (Ik −/−) at E18.5. **d:** Relative volume of the germinal zone (GZ) examined by measuring the proliferative area observed after BrdU administration. This result confirms the increased GZ volume observed in *Ikaros*$^{-/-}$ embryos with respect to wt embryos. Results are expressed as the relative volume (%) of each area in relation to total brain volume. Results represent the mean of four to six animals ± SEM. Statistical analysis was by Student's *t*-test. *$P < 0.05$ relative to wt. **e,f:** MAP2ab immunohistochemistry performed in coronal sections of wt and *Ikaros*$^{-/-}$ (Ik −/−) embryos at E18.5 shows the differences in volumes of GZ and MZ between the two genotypes. Scale bar = 450 μm.

parvalbumin-positive and cholinergic interneurons (Fig. 7j,k, respectively). Taken together, these results showed that Ikaros regulates the generation of striatal projection neurons that express ENK. To confirm these results in vitro, we overexpressed Ikaros-1 in striatal primary cultures. Double immunocytochemistry showed that Ikaros-1 induced the differentiation of NPCs to ENK-positive striatal projection neurons, insofar as cells overexpressing this transcription factor presented greater colocalization with ENK- and calbindin-positive neurons than did the eGFP-overexpressing control cells (Fig. 8a–j).

Ikaros-1 acts downstream of Dlx-gene expression and independently of Ebf-1

Many transcription factors affect the development of striatal neuronal populations following sequential expression patterns. In particular, Dlx-1 and -2 are involved in the neurogenesis of late-born striatal neurons (Anderson et al., 1997; Yun et al., 2002). Because Ikaros also participates in the late wave of striatal neurogenesis, it was plausible that these transcription factors could be acting on the same NPCs. Thus, we examined the expression of Dlx-2 and Dlx-5 in *Ikaros*$^{-/-}$ embryos. We observed no differences in the distribution or levels of Dlx transcription factors in wt mice at E15.5 or E18.5 (Fig. 9a–h). These findings indicate that Ikaros was either downstream or independent of *Dlx* genes. Therefore, we next examined the expression of Ikaros in *Dlx-1/2* double-knockout mice. Our results demonstrated that Ikaros expression was strongly reduced in *Dlx-1/2* double-knockout mice at E18.5 (Fig. 9i,j), suggesting that Ikaros is downstream of Dlx. These results have also been observed at E15.5, reinforcing our hypothesis (Long et al., 2009). *Dlx-1/2* double-knockout mice have lower MZ (Anderson et al., 1997), so it could be that Ikaros was absent because of LGE atrophy. However, Ebf-1 expression, another LGE-specific transcription factor, was preserved in the modified MZ of *Dlx-1/2* double-knockout mice (Fig. 9k,l). In addition, the analysis of Ikaros expression in Dlx-5/6-GFP mice showed that all Ikaros-expressing cells colocalize with GFP-positive cells, confirming that this transcription factor was located in the same NPC lineage (Fig. 9m–o).

We next studied the relationship between Ikaros-1 and Ebf-1. First, we analyzed the expression of Ebf-1 in *Ikaros*$^{-/-}$

Figure 6. Ikaros is a critical factor for the second wave of striatal neurogenesis. **a–c:** Birth-dating experiments were performed by injecting BrdU in *Ikaros*$^{+/-}$ pregnant mice at E12.5 (a), E14.5 (b), and E16.5 (c) and analyzed at E18.5. *Ikaros*$^{-/-}$ embryos (Ik −/−) show a reduction in the density of new postmitotic cells (BrdU-positive cells × 10^3/mm^3) generated at E14.5 in the MZ. **d:** Analysis of the number of proliferating cells in the GZ of E14.5 embryos that were injected with BrdU and evaluated 30 minutes later. *Ikaros*$^{-/-}$ embryos showed increased density of BrdU-positive cells in the GZ. a–d: Results are expressed as the mean of three or four embryos, and error bars represent the SEM. Statistical analysis was by Student's *t*-test. *$P < 0.05$ relative to wt. **e,f:** Fluorescent photomicrographs of BrdU immunohistochemistry following a short BrdU pulse at E14.5 in wt and *Ikaros*$^{-/-}$ (Ik −/−) embryos. Arrows indicate proliferating BrdU-positive cells in the GZ. **g,h:** Cell death analysis performed in coronal sections of wt and Ikaros-deficient embryos (Ik −/−) at E18.5. There are no differences in the number of TUNEL-positive cells between the two genotypes. Arrows indicate TUNEL-positive cells. **i,j:** Fluorescent photomicrograph of GFAP immunohistochemistry performed in coronal sections of adult wt and Ikaros$^{-/-}$ (Ik −/−) mice. Scale bars = 150 μm in f (applies to e,f); 150 μm in h (applies to g,h); 450 μm in i (applies to i,j).

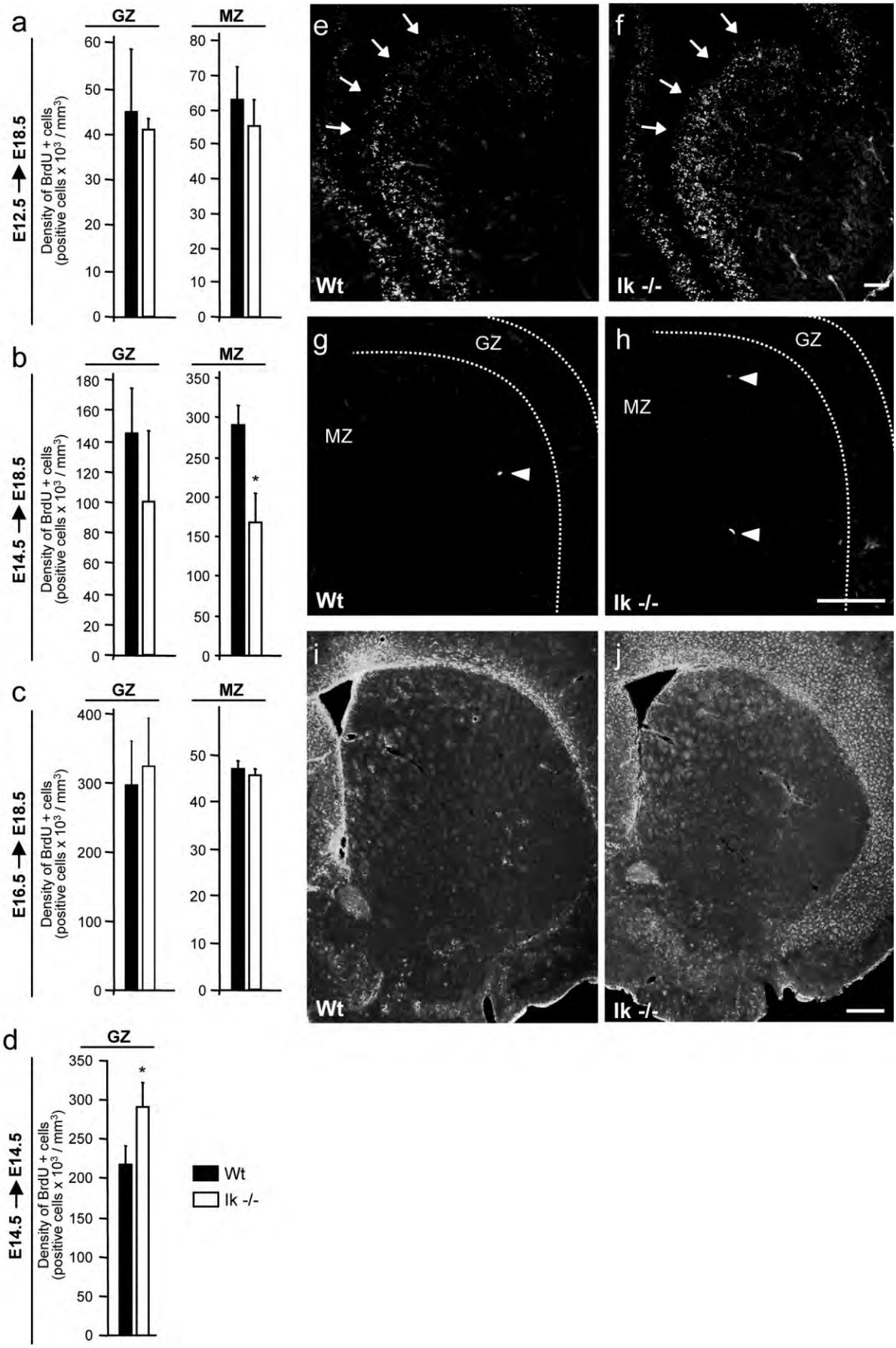
a
GZ
MZ
E12.5 → E18.5
Density of BrdU + cells (positive cells x 10³ / mm³)
b
E14.5 → E18.5
*
c
E16.5 → E18.5
d
E14.5 → E14.5
Wt
Ik -/-
e
f
g
h
i
j
Wt
Ik -/-
GZ
MZ

Figure 6

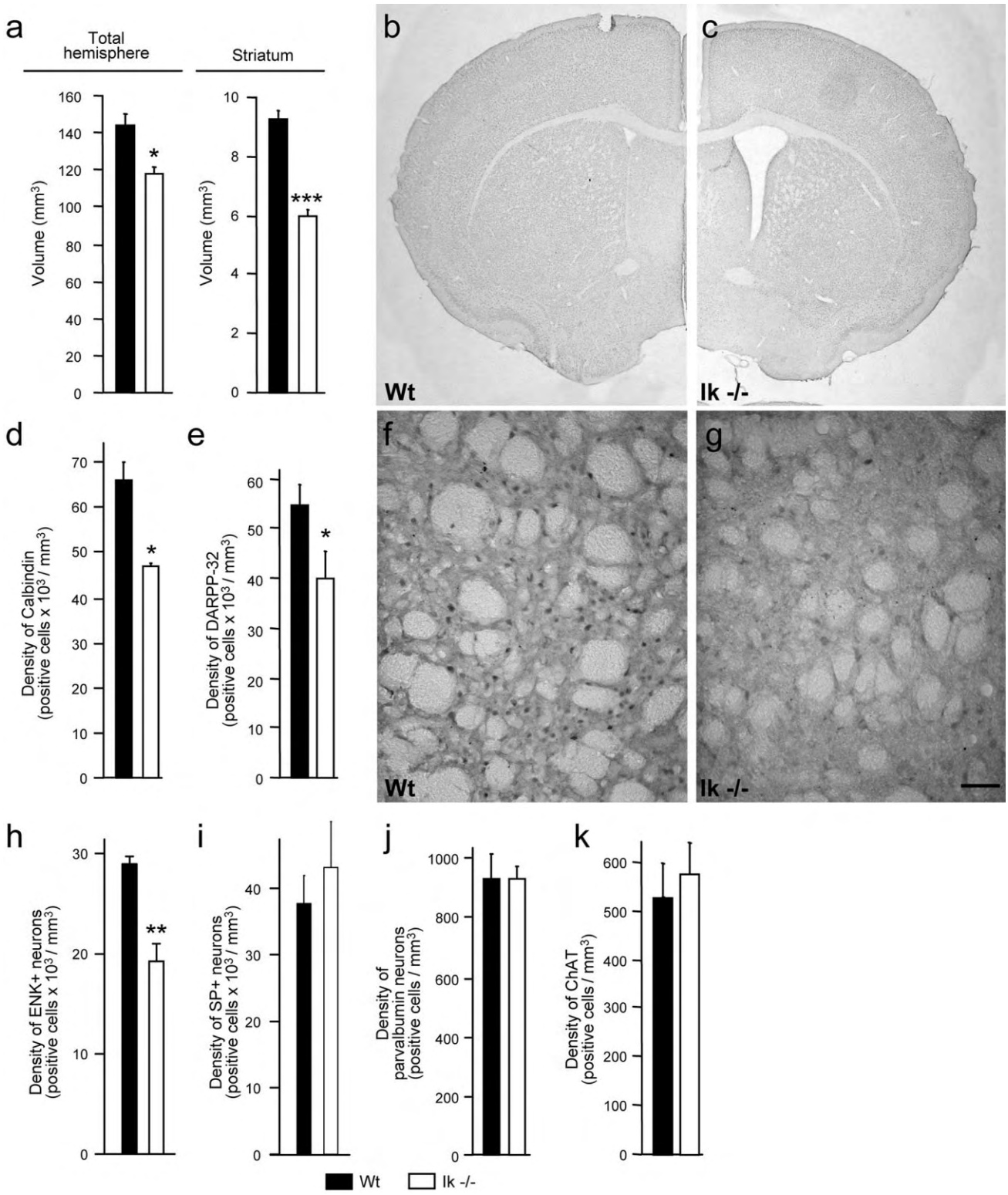

Figure 7

and wt mice at E15.5 and E18.5 (Fig. 10a–d). No differences were found in the levels of expression or in the distribution of Ebf-1 between both genotypes at any of the ages studied. Second, we analyzed the expression of Ikaros-1 in *Ebf-1*$^{-/-}$ and wt mice at E18.5. Consistently, no differences were found in the levels of expression of Ikaros in the absence of Ebf-1 (Fig. 10e,f). Taken together, these results suggest that Ikaros-1 and Ebf-1 are involved in the determination of striatal

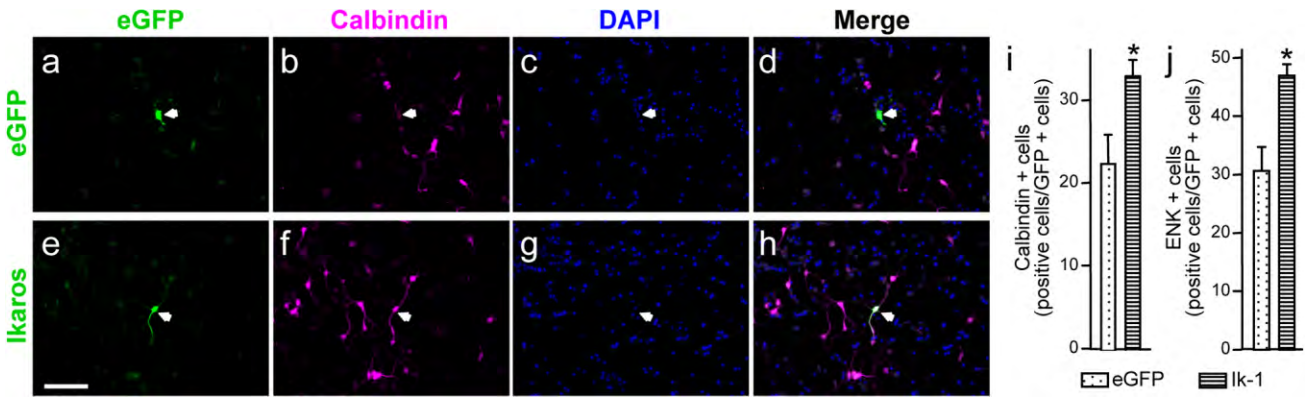

Figure 8. Overexpression of Ikaros-1 increases the determination of ENK-positive projecting neurons in LGE primary cultures. **a–h:** Representative photomicrographs showing double immunocytochemistry for eGFP and calbindin in primary cultures overexpressing eGFP (a–d) or Ikaros-1 (e–h). **i,j:** Quantification of the number of Ikaros-1- and eGFP-positive cells colocalizing with calbindin (i) and ENK (j). Note that Ikaros-1-overexpressing cells show higher levels of colocalization with both calbindin and ENK than the control cells overexpressing eGFP. Graph bars represent the percentage of positive cells for each marker from among the total number of eGFP-positive cells. Results are expressed as the mean of three or four LGE primary cultures transfected, and error bars represent the SEM. Statistical analysis was by Student's *t*-test. $*P < 0.05$ relative to eGFP-transfected primary cultures. Scale bar = 50 μm.

projection neurons following parallel but independent pathways.

DISCUSSION

NPCs from ganglionic eminences give rise to a broad range of neurons during telencephalic development (Brazel et al., 2003; Zaki et al., 2003; Guillemot, 2007). However, little is known about the regulation of these processes, in particular regarding cell cycle arrest and the specific neurogenesis of discrete striatal projection neuronal populations. Our present findings demonstrate that Ikaros induces cell cycle exit through the regulation of $p21^{Cip1/Waf1}$. This mechanism se-

Figure 7. Loss of Ikaros affects the development of striatal projecting neurons that express ENK. **a:** Absolute volumes corresponding to total hemisphere and striatum of adult wt and *Ikaros*$^{-/-}$ mice. **b,c:** NeuN immunohistochemistry performed in adult brain sections shows that *Ikaros*$^{-/-}$ mice have less striatal volume than wt mice. **d–k:** Histological characterization of neuronal populations in the striatum of adult *Ikaros*$^{-/-}$ mice (Ik −/−). d: The density of matrix striatal neurons was determined by counting the number of calbindin-positive neurons per cubic millimeter in the striatum of wt or *Ikaros*$^{-/-}$ mice. e: The density of striatal projection neurons was also counted as the number of DARPP-32-positive neurons per cubic millimeter in the striatum of wt or *Ikaros*$^{-/-}$ mice. f,g: Representative photomicrograph of DARPP-32 immunohistochemistry performed in adult wt and Ikaros$^{-/-}$ brains. h,i: Analysis of the density of the two populations of striatal projecting neurons: ENK-positive neurons (ENK; h) and SP-positive neurons (SP; i) in wt and Ikaros$^{-/-}$ mice. j,k: Analysis of the density of striatal interneurons, including GABAergic (j; parvalbumin-positive cells) and cholinergic (k; ChAT-positive cells) in wt and *Ikaros*$^{-/-}$ mice. a,d,e,h–k: Results are expressed as the mean of six animals, and error bars represent the SEM. Statistical analysis was by Student's *t*-test. $*P < 0.05$, $**P < 0.005$, $***P < 0.001$ relative to wt. Scale bar = 50 μm.

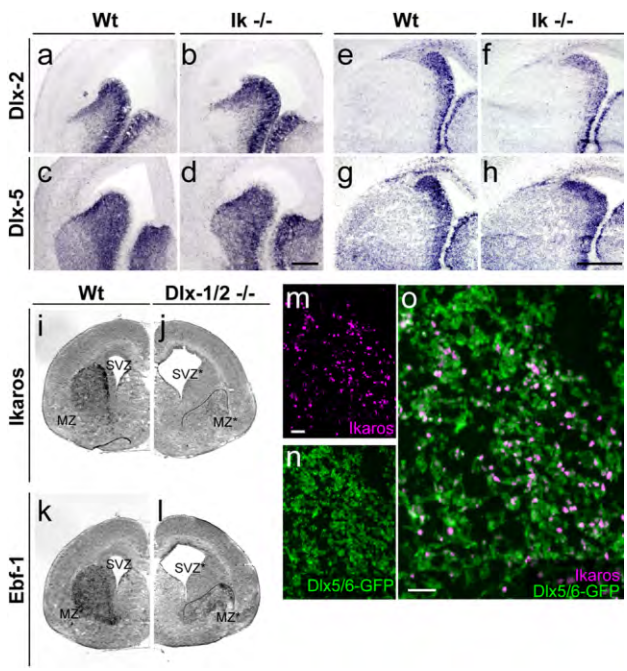

Figure 9. Ikaros expression is downstream of Dlx genes during striatal development. **a–h:** In situ hybridization analysis of the expression of Dlx-2 and Dlx-5 in wt and *Ikaros*$^{-/-}$ (Ik −/−) embryos at E15.5 (a–d) and E18.5 (e–h). There are no differences in the expression of these transcription factors between the two genotypes. **i–l:** Ikaros mRNA was not detected in the striatum of *Dlx-1/2*$^{-/-}$ at E18.5 (i,j), whereas Ebf-1 expression was preserved in the modified MZ of these mice at the same embryonic stage (k,l). **m–o:** Ikaros-1 is expressed in neurons of the Dlx5/6 lineage; double immunohistochemistry performed for Ikaros-1 and eGFP in Dlx-5/6-Cre-IRES-GFP transgenic mice at E18.5. Scale bars = 500 μm in d (applies to a–d); 500 μm in h (applies to e–h) 100 μm in o (applies to m–o).

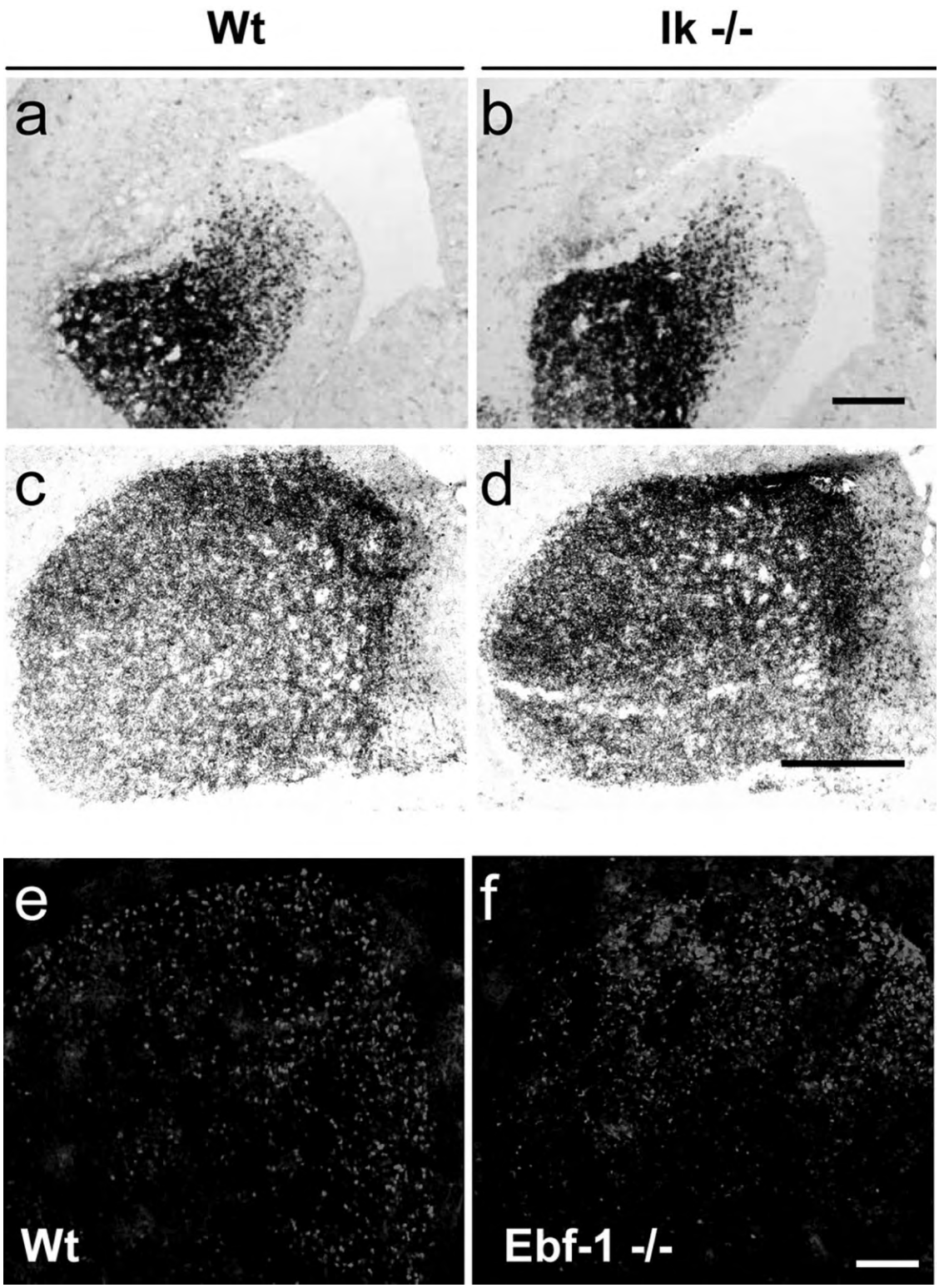

Figure 10. Ikaros-1 and Ebf-1 are independent factors during striatal development. **a–d:** In situ hybridization study to analyze the expression of Ebf-1 in wt and Ikaros$^{-/-}$ (Ik −/−) embryos at E15.5 (a,b) and E18.5 (c,d). There are no differences in the expression of Ebf-1 between the two genotypes. **e,f:** Analysis of the expression of Ikaros-1 in wt (e) and Ebf-1$^{-/-}$ (f) embryos at E18.8 by immunohistochemistry. There are no differences in the expression of Ikaros-1 between the two genotypes. Scale bars = 500 μm in b (applies to a,b); 500 μm in d (applies to c,d); 150 μ in f (applies to e,f).

lectively affects the late NPCs that give rise to the second wave of striatal neurogenesis. Consequently, *Ikaros*$^{-/-}$ mice have a reduced striatum and a deficit in the number of ENK-positive projecting neurons.

Ikaros-1 induces cell cycle arrest of late striatal progenitors

Several transcription factors act as cell-fate determinants during the final cell cycle of progenitor cells (Tanabe et al., 1998; Nguyen et al., 2006). Our present findings support the hypothesis that Ikaros-1 is an instructive factor that functions by regulating cell cycle arrest. First, and in agreement with earlier studies (Agoston et al., 2007), we found that the higher levels of Ikaros expression were detected at the SVZ–MZ boundary of the LGE, suggesting that this transcription factor is involved in the delimitation between the proliferating SVZ and the postmitotic MZ. Second, Ikaros-1 is expressed by βIII-tubulin-positive cells, labeling early postmitotic neurons during or immediately after the last mitotic cycle (Lee et al., 1990). Although it has been suggested that βIII-tubulin-positive cells become postmitotic before migration to their target area, our present findings point to the idea that a specific subset of NPCs of the SVZ migrates to the MZ, where they become postmitotic neurons through the influence of Ikaros-1. Consistently with this hypothesis, we found that Ikaros-1 overexpression reduced the number of proliferating precursors in neurosphere assay, whereas *Ikaros*$^{-/-}$-derived neurospheres increased proliferation. Moreover, overexpression of Ikaros-1 in NPCs and/or in striatal primary cultures induced the differentiation of neural precursors to postmitotic neurons. Although we observed that all Ikaros-1-overexpressing NPCs were negative for BrdU labelling after a short-term pulse, Ikaros colocalizes with BrdU-positive cells in the LGE after long-term treatments (18 hours; Agoston et al., 2007). This is consistent with the idea that Ikaros is expressed by young postmitotic neurons, insofar as a large pulse of BrdU is useful for detecting cells that leave the cell cycle (Mason et al., 2005). Taken together, all these findings indicate that Ikaros-1 regulates the transition from NPCs to postmitotic neurons. Interestingly, our results show that *Ikaros*$^{-/-}$ mice retain NPCs at the GZ, which can finally differentiate into glial cells, as suggested by the increase of astrocytes observed in these mice in adulthood, especially in the cerebral cortex. It has been demonstrated that NPCs first generate neurons and that later these NPCs terminaly differentiate into glial cells. Thus, the lack of Ikaros could reduce neurogenesis and favor astroglial determination. In fact, astrocytes in the cerebral cortex derive from subpallial Dlx-2-expressing cells (Marshall and Goldman, 2002). However, further experiments are needed to verify whether the increase of astrocytes is directly or indirectly related to Ikaros loss.

It has been shown that Ikaros-1 participates in regulation of the cell cycle by leading to the growth arrest of hematopoietic stem cells throughout up-regulation of $p27^{Kip1}$ (Kathrein et al., 2005). In addition, CDKi, such as $p21^{Cip1/Waf1}$ and $p27^{Kip1}$, have important functions not only in hematopoietic stem cell homeostasis (Ezoe et al., 2004), but also in maintaining neural stem cells (van Lookeren and Gill, 1998; Doetsch et al., 2002; Kippin et al., 2005). Here we show that Ikaros-1 induces cell cycle exit by the up-regulation of $p21^{Cip1/Waf1}$, but not of $p27^{Kip1}$, in NPCs. The effect of Ikaros-1 on $p21^{Cip1/Waf1}$ mRNA and protein suggests a direct effect, as was suggested for $p27^{Kip1}$ in the hematopoietic system (Kathrein et al., 2005). In fact, we found that $p21^{Cip1/Waf1}$ promoter has one predicted binding site for Ikaros (TFSEARCH program, version 1.3; 1995, Yutaka Akiyama, Kyoto University). Therefore, $p21^{Cip1/Waf1}$ and $p27^{Kip1}$ are direct targets of Ikaros that could be regulated specifically depending on the acting system. Moreover, we show that Ikaros-1 cannot induce cell cycle arrest in *p21*$^{-/-}$-derived NPCs. $p21^{Cip1/Waf1}$ acts in the G_1 phase of the cell cycle and delays or blocks the progression of the cell into S phase (Sherr and Roberts, 1999). In addition, it has been reported that the exit of neural cells from the cell cycle appears to occur at the restriction point of the G1 phase (Zetterberg et al., 1995; Edlund and Jessell, 1999; Pechnick et al., 2008). Thus, it seems plausible that Ikaros-1 causes higher levels of the CDKi $p21^{Cip1/Waf1}$, which, in turn, induce neurogenesis of NPCs. Moreover, we show that this is a specific mechanism, in that we found no changes in the expression of the Notch family members or in the levels of Notch1 intracellular domain after Ikaros-1 overexpression, another pathway that is involved in Ikaros-mediated regulation of proliferative processes (Demarest et al., 2008).

Ikaros-1 acts as a positive regulator of the second wave of striatal neurogenesis

During striatal development, late NPCs give rise to neurons of the matrix compartment, which can become ENK- or SP-positive neurons (van der Kooy and Fishell, 1987). Our results demonstrate that Ikaros-1 is essential for the earlier stages of the second wave of striatal neurogenesis. Moreover, Ikaros loss produces a reduction in the number of striatal projection neurons and, particularly, those that express ENK. Thus, similarly to some other transcription factors (Tanabe et al., 1998; Canzoniere et al., 2004; Paris et al., 2006), Ikaros-1 may have a dual role, regulating the cell cycle arrest of striatal NPCs and inducing the differentiation of ENK-positive projection neurons. It has been previously described that Ikaros participates in the differentiation of ENK-positive neurons by direct interaction with the ENK promoter (Dobi et al., 1997; Agoston et al., 2007).

However, in the present work, we show that Ikaros increases the number not only of ENK-positive neurons but also of calbindin-positive neurons in primary striatal cultures, demonstrating that it is acting at the promoter level and on differentiation of NPCs. Interestingly, overexpression of Ikaros-1 in cerebellum-derived NPCs increased the levels of ENK expression but was not effective for inducing other striatal markers (data not shown). Thus, other, context-dependent factors could be also important for the role of Ikaros-1 during development.

Results obtained from Ikaros mutant models indicate that this transcription factor is critical for the development of a specific subpopulation of striatal ENK-positive neurons, in that not all ENK-positive neurons were depleted in both mutant mice (present results and Agoston et al., 2007). Thus, other factors should participate in the development of these neurons. In keeping with this view, Ikaros-dominant negative mice showed more severe striatal affection than *Ikaros*$^{-/-}$ mice (Agoston et al., 2007), suggesting the participation of other Ikaros-related factors. We observed that Helios is also expressed in the LGE during development (Crespo et al., in preparation), which favors a role for this factor. Moreover, within the hematopoietic system, compensatory mechanisms have been described between Ikaros and Helios (Zhang et al., 2007). However, our findings show that Ikaros and Helios are expressed by different cells and that the latter is equally expressed in the striatum of wt and *Ikaros*$^{-/-}$ embryos during development, suggesting a lack of compensation (Crespo et al., in preparation). Nevertheless, it has been described that other factors may regulate the expression of ENK (Agoston and Dobi, 2000), which could compensate for the lack of Ikaros at later stages of matrix formation.

A model for development of striatal projecting neurons

It has recently been shown that Ikaros regulates the early competence of retinal NPCs, suggesting that similar strategies may operate to generate neurons in other brain areas (Elliott et al., 2008). However, the demonstration that Ikaros-1 regulates late striatal neurogenesis argues against this hypothesis, indicating that Ikaros family members act by selective mechanisms in different parts of the nervous system, depending on determined contexts.

Specific genes coordinate intrinsic programs to produce different progeny (Merkle and Alvarez-Buylla, 2006). Thus, we next examined the relationship of Ikaros with other factors involved in striatal development. Dlx-1/2 are involved in the differentiation of NPCs that produce the late wave of striatal neurogenesis (Anderson et al., 1997), which is the most affected by Ikaros loss (present results). Dlx-1/2 are expressed by NPCs in the GZ (Bulfone et al., 1993; Eisenstat et al., 1999), which migrate to the MZ (Nery et al., 2003). Within the MZ, Dlx-1/2 expression is extinguished, whereas Dlx-5/6 are expressed in more mature cells (Eisenstat et al., 1999). Our findings demonstrated that Ikaros-1 exerts its effect downstream of Dlx factors, insofar as its expression disappeared in Dlx-1/2 knockout (present results and Long et al., 2009). These nuclear regulators expressed in NPCs may control not only fate determinations but also migration during development (Cobos et al., 2007). Thus, Ikaros-1 could also participate in the control of NPC migration. However, this is unlikely, because Ikaros-1 expression is downstream of Dlx-5/6-positive migratory NPCs and is located only in the postmigratory MZ.

Ebf-1 is highly expressed in the matrix compartment of the MZ (Garel et al., 1999) and regulates cell cycle exit and neural differentiation (Garcia-Dominguez et al., 2003). Thus, a parallelism between Ebf-1 and Ikaros-1 can be postulated. However, Ikaros-1 participates in the development of ENK-positive neurons, whereas Ebf-1 is a lineage-specific factor essential for the differentiation of early-generated SP neurons (Lobo et al., 2006). No effect of the expression of Ikaros-1 and Ebf-1 is seen in either of the opposed null mutant mice. This finding points to the existence of independent mechanisms for generating both striatonigral and striatopallidal populations of the matrix compartment. Our results also showed that Ikaros-1 depends on Dlx gene expression, whereas Ebf-1 is preserved in the modified MZ of Dlx1/2 double mutant mice. These findings allow us to propose a model for the development of striatal projecting neurons located in the matrix compartment. A first type of Mash1-negative/Dlx-negative striatal NPCs has been described (Yun et al., 2002). Mash1 is required for the generation of a second type of Dlx-negative/Mash1-positive NPC (Yun et al., 2002), which could directly or indirectly express Ebf-1 to produce the SP-positive neurons in the matrix compartment. Another subset of Mash-positive NPCs progresses toward Dlx-positive NPCs (Poitras et al., 2007). Within the MZ, Dlx-5/6-positive NPCs express Ikaros-1, which will induce striatal neurogenesis of ENK-positive neurons. In conclusion, Ikaros-1 regulates cell cycle exit of specific Dlx-derived NPCs that will generate a subset of striatal ENK-positive neurons localized in the matrix compartment.

ACKNOWLEDGMENTS

We thank M.T. Muñoz, A. López, T. Gil, and M. Bonete for technical support and Dr. Maria Calvo and Anna Bosch from the confocal microscopy unit at the Serveis Científico-Tècnics (Universitat de Barcelona) for their support and advice on confocal techniques. We also thank Dr. K. Campbell for providing Dlx5/6Cre-IRES-EGFP trans-

genic mice, Dr. Rudolf Grosschedl for Ebf1$^{-/-}$ mice, and Dr. Susan Winandy for Ikaros constructs. We are also very grateful to Robin Rycroft for the English language revision.

LITERATURE CITED

Agoston DV, Dobi A. 2000. Complexity of transcriptional control in neuropeptide gene expression; enkephalin gene regulation during neurodevelopment. Biochem Soc Trans 28:446–451.

Agoston DV, Szemes M, Dobi A, Palkovits M, Georgopoulos K, Gyorgy A, Ring MA. 2007. Ikaros is expressed in developing striatal neurons and involved in enkephalinergic differentiation. J Neurochem 102:1805–1816.

Alvarez-Buylla A, Seri B, Doetsch F. 2002. Identification of neural stem cells in the adult vertebrate brain. Brain Res Bull 57: 751–758.

Anderson SA, Qiu M, Bulfone A, Eisenstat DD, Meneses J, Pedersen R, Rubenstein JL. 1997. Mutations of the homeobox genes Dlx-1 and Dlx-2 disrupt the striatal subventricular zone and differentiation of late born striatal neurons. Neuron 19: 27–37.

Bertrand N, Castro DS, Guillemot F. 2002. Proneural genes and the specification of neural cell types. Nat Rev Neurosci 3:517–530.

Bhagwandin A, Fuxe K, Manger PR. 2006. Choline acetyltransferase immunoreactive cortical interneurons do not occur in all rodents: a study of the phylogenetic occurrence of this neural characteristic. J Chem Neuroanat 32:208–216.

Binder LI, Frankfurter A, Rebhun LI. 1986. Differential localization of MAP-2 and tau in mammalian neurons in situ. Ann N Y Acad Sci 466:145–166.

Bloomfield C, O'Donnell P, French SJ, Totterdell S. 2007. Cholinergic neurons of the adult rat striatum are immunoreactive for glutamatergic *n*-methyl-d-aspartate 2d but not *n*-methyl-d-aspartate 2c receptor subunits. Neuroscience 150:639–646.

Bosch M, Pineda JR, Sunol C, Petriz J, Cattaneo E, Alberch J, Canals JM. 2004. Induction of GABAergic phenotype in a neural stem cell line for transplantation in an excitotoxic model of Huntington's disease. Exp Neurol 190:42–58.

Brazel CY, Romanko MJ, Rothstein RP, Levison SW. 2003. Roles of the mammalian subventricular zone in brain development. Prog Neurobiol 69:49–69.

Brenner M, Kisseberth WC, Su Y, Besnard F, Messing A. 1994. GFAP promoter directs astrocyte-specific expression in transgenic mice. J Neurosci 14:1030–1037.

Brugarolas J, Chandrasekaran C, Gordon JI, Beach D, Jacks T, Hannon GJ. 1995. Radiation-induced cell cycle arrest compromised by p21 deficiency. Nature 377:552–557.

Bulfone A, Puelles L, Porteus MH, Frohman MA, Martin GR, Rubenstein JL. 1993. Spatially restricted expression of Dlx-1, Dlx-2 (Tes-1), Gbx-2, and Wnt-3 in the embryonic day 12.5 mouse forebrain defines potential transverse and longitudinal segmental boundaries. J Neurosci 13:3155–3172.

Caillard O, Moreno H, Schwaller B, Llano I, Celio MR, Marty A. 2000. Role of the calcium-binding protein parvalbumin in short-term synaptic plasticity. Proc Natl Acad Sci U S A 97: 13372–13377.

Campbell K. 2003. Dorsal-ventral patterning in the mammalian telencephalon. Curr Opin Neurobiol 13:50–56.

Canals JM, Checa N, Marco S, Akerud P, Michels A, Perez-Navarro E, Tolosa E, Arenas E, Alberch J. 2001. Expression of brain-derived neurotrophic factor in cortical neurons is regulated by striatal target area. J Neurosci 21:117–124.

Canals JM, Pineda JR, Torres-Peraza JF, Bosch M, Martin-Ibanez R, Munoz MT, Mengod G, Ernfors P, Alberch J. 2004. Brain-derived neurotrophic factor regulates the onset and severity of motor dysfunction associated with enkephalinergic neuronal degeneration in Huntington's disease. J Neurosci 24: 7727–7739.

Canudas AM, Pezzi S, Canals JM, Pallas M, Alberch J. 2005. Endogenous brain-derived neurotrophic factor protects dopaminergic nigral neurons against transneuronal degeneration induced by striatal excitotoxic injury. Brain Res Mol Brain Res 134:147–154.

Canzoniere D, Farioli-Vecchioli S, Conti F, Ciotti MT, Tata AM, Augusti-Tocco G, Mattei E, Lakshmana MK, Krizhanovsky V, Reeves SA, Giovannoni R, Castano F, Servadio A, Ben Arie N, Tirone F. 2004. Dual control of neurogenesis by PC3 through cell cycle inhibition and induction of Math1. J Neurosci 24: 3355–3369.

Cleary MA, Uboha N, Picciotto MR, Beech RD. 2006. Expression of ezrin in glial tubes in the adult subventricular zone and rostral migratory stream. Neuroscience 143:851–861.

Cobos I, Borello U, Rubenstein JL. 2007. Dlx transcription factors promote migration through repression of axon and dendrite growth. Neuron 54:873–888.

Demarest RM, Ratti F, Capobianco AJ. 2008. It's T-ALL about Notch. Oncogene 27:5082–5091.

Dobi A, Palkovits M, Ring MA, Eitel A, Palkovits CG, Lim F, Agoston DV. 1997. Sample and probe: a novel approach for identifying development-specific cis-elements of the enkephalin gene. Brain Res Mol Brain Res 52:98–111.

Doetsch F, Verdugo JM, Caille I, Alvarez-Buylla A, Chao MV, Casaccia-Bonnefil P. 2002. Lack of the cell-cycle inhibitor p27^{Kip1} results in selective increase of transit-amplifying cells for adult neurogenesis. J Neurosci 22:2255–2264.

Dolbeare F, Gratzner H, Pallavicini MG, Gray JW. 1983. Flow cytometric measurement of total DNA content and incorporated bromodeoxyuridine. Proc Natl Acad Sci U S A 80:5573–5577.

Edlund T, Jessell TM. 1999. Progression from extrinsic to intrinsic signaling in cell fate specification: a view from the nervous system. Cell 96:211–224.

Eisenstat DD, Liu JK, Mione M, Zhong W, Yu G, Anderson SA, Ghattas I, Puelles L, Rubenstein JL. 1999. DLX-1, DLX-2, and DLX-5 expression define distinct stages of basal forebrain differentiation. J Comp Neurol 414:217–237.

Elliott J, Jolicoeur C, Ramamurthy V, Cayouette M. 2008. Ikaros confers early temporal competence to mouse retinal progenitor cells. Neuron 60:26–39.

Ezoe S, Matsumura I, Satoh Y, Tanaka H, Kanakura Y. 2004. Cell cycle regulation in hematopoietic stem/progenitor cells. Cell Cycle 3:314–318.

Ezzat S, Mader R, Fischer S, Yu S, Ackerley C, Asa SL. 2006. An essential role for the hematopoietic transcription factor Ikaros in hypothalamic-pituitary-mediated somatic growth. Proc Natl Acad Sci U S A 103:2214–2219.

Flames N, Long JE, Garratt AN, Fischer TM, Gassmann M, Birchmeier C, Lai C, Rubenstein JL, Marin O. 2004. Short- and long-range attraction of cortical GABAergic interneurons by neuregulin-1. Neuron 44:251–261.

Garcia-Dominguez M, Poquet C, Garel S, Charnay P. 2003. Ebf gene function is required for coupling neuronal differentiation and cell cycle exit. Development 130:6013–6025.

Garel S, Marin F, Grosschedl R, Charnay P. 1999. Ebf1 controls early cell differentiation in the embryonic striatum. Development 126:5285–5294.

Georgopoulos K. 2002. Haematopoietic cell-fate decisions, chromatin regulation and ikaros. Nat Rev Immunol 2:162–174.

Georgopoulos K, Moore DD, Derfler B. 1992. Ikaros, an early lymphoid-specific transcription factor and a putative mediator for T cell commitment. Science 258:808–812.

Georgopoulos K, Bigby M, Wang JH, Molnar A, Wu P, Winandy S, Sharpe A. 1994. The Ikaros gene is required for the development of all lymphoid lineages. Cell 79:143–156.

Gerfen CR. 1992. The neostriatal mosaic: multiple levels of compartmental organization. Trends Neurosci 15:133–139.

Gomez-del-Arco P, Maki K, Georgopoulos K. 2004. Phosphorylation controls Ikaros's ability to negatively regulate the G_1-S transition. Mol Cell Biol 24:2797–2807.

Gratacos E, Perez-Navarro E, Tolosa E, Arenas E, Alberch J. 2001. Neuroprotection of striatal neurons against kainate excitotoxicity by neurotrophins and GDNF family members. J Neurochem 78:1287–1296.

Guillemot F. 2007. Cell fate specification in the mammalian telencephalon. Prog Neurobiol 83:37–52.

Gundersen HJ, Bendtsen TF, Korbo L, Marcussen N, Moller A, Nielsen K, Nyengaard JR, Pakkenberg B, Sorensen FB, Vesterby A. 1988. Some new, simple and efficient stereological methods and their use in pathological research and diagnosis. APMIS 96:379–394.

Haverkamp S, Wassle H. 2000. Immunocytochemical analysis of the mouse retina. J Comp Neurol 424:1–23.

Hirano K, Ihara E, Hirano M, Nishimura J, Nawata H, Kanaide H. 2004. Facilitation of proteasomal degradation of $p27^{Kip1}$ by N-terminal cleavage and their sequence requirements. FEBS Lett 574:111–115.

Jaime M, Pujol MJ, Serratosa J, Pantoja C, Canela N, Casanovas O, Serrano M, Agell N, Bachs O. 2002. The $p21^{Cip1}$ protein, a cyclin inhibitor, regulates the levels and the intracellular localization of CDC25A in mice regenerating livers. Hepatology 35:1063–1071.

Kathrein KL, Lorenz R, Innes AM, Griffiths E, Winandy S. 2005. Ikaros induces quiescence and T-cell differentiation in a leukemia cell line. Mol Cell Biol 25:1645–1654.

Kippin TE, Martens DJ, van der KD. 2005. p21 Loss compromises the relative quiescence of forebrain stem cell proliferation leading to exhaustion of their proliferation capacity. Genes Dev 19:756–767.

Lee MK, Tuttle JB, Rebhun LI, Cleveland DW, Frankfurter A. 1990. The expression and posttranslational modification of a neuron-specific beta-tubulin isotype during chick embryogenesis. Cell Motil Cytoskeleton 17:118–132.

Lin H, Grosschedl R. 1995. Failure of B-cell differentiation in mice lacking the transcription factor EBF. Nature 376:263–267.

Lobo MK, Karsten SL, Gray M, Geschwind DH, Yang XW. 2006. FACS-array profiling of striatal projection neuron subtypes in juvenile and adult mouse brains. Nat Neurosci 9:443–452.

Long JE, Swan C, Liang WS, Cobos I, Potter GB, Rubenstein JL. 2009. Dlx1&2 and Mash1 transcription factors control striatal patterning and differentiation through parallel and overlapping pathways. J Comp Neurol 512:556–572.

Magaud JP, Sargent I, Mason DY. 1988. Detection of human white cell proliferative responses by immunoenzymatic measurement of bromodeoxyuridine uptake. J Immunol Methods 106:95–100.

Magaud JP, Sargent I, Clarke PJ, Ffrench M, Rimokh R, Mason DY. 1989. Double immunocytochemical labeling of cell and tissue samples with monoclonal anti-bromodeoxyuridine. J Histochem Cytochem 37:1517–1527.

Marshall CA, Goldman JE. 2002. Subpallial Dlx2-expressing cells give rise to astrocytes and oligodendrocytes in the cerebral cortex and white matter. J Neurosci 22:9821–9830.

Martin-Ibanez R, Urban N, Sergent-Tanguy S, Pineda JR, Garrido-Clua N, Alberch J, Canals JM. 2007. Interplay of leukemia inhibitory factor and retinoic acid on neural differentiation of mouse embryonic stem cells. J Neurosci Res 85:2686–2701.

Mason HA, Rakowiecki SM, Raftopoulou M, Nery S, Huang Y, Gridley T, Fishell G. 2005. Notch signaling coordinates the patterning of striatal compartments. Development 132:4247–4258.

Merkle FT, Alvarez-Buylla A. 2006. Neural stem cells in mammalian development. Curr Opin Cell Biol 18:704–709.

Molnar A, Georgopoulos K. 1994. The Ikaros gene encodes a family of functionally diverse zinc finger DNA-binding proteins. Mol Cell Biol 14:8292–8303.

Molnar A, Wu P, Largespada DA, Vortkamp A, Scherer S, Copeland NG, Jenkins NA, Bruns G, Georgopoulos K. 1996. The Ikaros gene encodes a family of lymphocyte-restricted zinc finger DNA binding proteins, highly conserved in human and mouse. J Immunol 156:585–592.

Nery S, Corbin JG, Fishell G. 2003. Dlx2 progenitor migration in wild type and Nkx2.1 mutant telencephalon. Cereb Cortex 13:895–903.

Nguyen L, Besson A, Roberts JM, Guillemot F. 2006. Coupling cell cycle exit, neuronal differentiation and migration in cortical neurogenesis. Cell Cycle 5:2314–2318.

Pallante BA, Duignan I, Okin D, Chin A, Bressan MC, Mikawa T, Edelberg JM. 2007. Bone marrow $Oct3/4^+$ cells differentiate into cardiac myocytes via age-dependent paracrine mechanisms. Circ Res 100:e1–11.

Paris M, Wang WH, Shin MH, Franklin DS, Andrisani OM. 2006. Homeodomain transcription factor Phox2a, via cyclic AMP-mediated activation, induces $p27^{Kip1}$ transcription, coordinating neural progenitor cell cycle exit and differentiation. Mol Cell Biol 26:8826–8839.

Pechnick RN, Zonis S, Wawrowsky K, Pourmorady J, Chesnokova V. 2008. p21Cip1 restricts neuronal proliferation in the subgranular zone of the dentate gyrus of the hippocampus. Proc Natl Acad Sci U S A 105:1358–1363.

Perez-Navarro E, Arenas E, Reiriz J, Calvo N, Alberch J. 1996. Glial cell line-derived neurotrophic factor protects striatal calbindin-immunoreactive neurons from excitotoxic damage. Neuroscience 75:345–352.

Perez-Navarro E, Alberch J, Neveu I, Arenas E. 1999. Brain-derived neurotrophic factor, neurotrophin-3 and neurotrophin-4/5 differentially regulate the phenotype and prevent degenerative changes in striatal projection neurons after excitotoxicity in vivo. Neuroscience 91:1257–1264.

Poitras L, Ghanem N, Hatch G, Ekker M. 2007. The proneural determinant MASH1 regulates forebrain Dlx1/2 expression through the I12b intergenic enhancer. Development 134:1755–1765.

Qiu M, Bulfone A, Ghattas I, Meneses JJ, Christensen L, Sharpe PT, Presley R, Pedersen RA, Rubenstein JL. 1997. Role of the Dlx homeobox genes in proximodistal patterning of the branchial arches: mutations of Dlx-1, Dlx-2, and Dlx-1 and -2 alter morphogenesis of proximal skeletal and soft tissue structures derived from the first and second arches. Dev Biol 185:165–184.

Rebollo A, Schmitt C. 2003. Ikaros, Aiolos and Helios: transcription regulators and lymphoid malignancies. Immunol Cell Biol 81:171–175.

Schaeren-Wiemers N, Gerfin-Moser A. 1993. A single protocol to detect transcripts of various types and expression levels in neural tissue and cultured cells: in situ hybridization using digoxigenin-labelled cRNA probes. Histochemistry 100:431–440.

Serrats J, Artigas F, Mengod G, Cortes R. 2003. $GABA_B$ receptor mRNA in the raphe nuclei: co-expression with serotonin transporter and glutamic acid decarboxylase. J Neurochem 84:743–752.

Sherr CJ, Roberts JM. 1999. CDK inhibitors: positive and negative regulators of G1-phase progression. Genes Dev 13:1501–1512.

Song DD, Harlan RE. 1994a. Genesis and migration patterns of neurons forming the patch and matrix compartments of the rat striatum. Brain Res Dev Brain Res 83:233–245.

Song DD, Harlan RE. 1994b. The development of enkephalin and substance P neurons in the basal ganglia: insights into neos-

triatal compartments and the extended amygdala. Brain Res Dev Brain Res 83:247–261.

Stenman J, Toresson H, Campbell K. 2003. Identification of two distinct progenitor populations in the lateral ganglionic eminence: implications for striatal and olfactory bulb neurogenesis. J Neurosci 23:167–174.

Sun L, Goodman PA, Wood CM, Crotty ML, Sensel M, Sather H, Navara C, Nachman J, Steinherz PG, Gaynon PS, Seibel N, Vassilev A, Juran BD, Reaman GH, Uckun FM. 1999. Expression of aberrantly spliced oncogenic ikaros isoforms in childhood acute lymphoblastic leukemia. J Clin Oncol 17:3753–3766.

Tanabe Y, William C, Jessell TM. 1998. Specification of motor neuron identity by the MNR2 homeodomain protein. Cell 95: 67–80.

Tokunaga A, Kohyama J, Yoshida T, Nakao K, Sawamoto K, Okano H. 2004. Mapping spatio-temporal activation of Notch signaling during neurogenesis and gliogenesis in the developing mouse brain. J Neurochem 90:142–154.

Toresson H, Campbell K. 2001. A role for Gsh1 in the developing striatum and olfactory bulb of Gsh2 mutant mice. Development 128:4769–4780.

Torres-Peraza J, Pezzi S, Canals JM, Gavalda N, Garcia-Martinez JM, Perez-Navarro E, Alberch J. 2007. Mice heterozygous for neurotrophin-3 display enhanced vulnerability to excitotoxicity in the striatum through increased expression of N-methyl-D-aspartate receptors. Neuroscience 144:462–471.

van der Kooy D, Fishell G. 1987. Neuronal birthdate underlies the development of striatal compartments. Brain Res 401:155–161.

van Lookeren CM, Gill R. 1998. Tumor-suppressor p53 is expressed in proliferating and newly formed neurons of the embryonic and postnatal rat brain: comparison with expression of the cell cycle regulators p21Waf1/Cip1, $p27^{Kip1}$, p57Kip2, p16Ink4a, cyclin G1, and the proto-oncogene Bax. J Comp Neurol 397:181–198.

Wang JH, Nichogiannopoulou A, Wu L, Sun L, Sharpe AH, Bigby M, Georgopoulos K. 1996. Selective defects in the development of the fetal and adult lymphoid system in mice with an Ikaros null mutation. Immunity 5:537–549.

Willett CE, Kawasaki H, Amemiya CT, Lin S, Steiner LA. 2001. Ikaros expression as a marker for lymphoid progenitors during zebrafish development. Dev Dyn 222:694–698.

Yasuda Y, Tateishi N, Shimoda T, Satoh S, Ogitani E, Fujita S. 2004. Relationship between S100β and GFAP expression in astrocytes during infarction and glial scar formation after mild transient ischemia. Brain Res 1021:20–31.

Yoshida T, Ng SY, Zuniga-Pflucker JC, Georgopoulos K. 2006. Early hematopoietic lineage restrictions directed by Ikaros. Nat Immunol 7:382–391.

Yun K, Fischman S, Johnson J, Hrabe de AM, Weinmaster G, Rubenstein JL. 2002. Modulation of the notch signaling by Mash1 and Dlx1/2 regulates sequential specification and differentiation of progenitor cell types in the subcortical telencephalon. Development 129:5029–5040.

Yun K, Garel S, Fischman S, Rubenstein JL. 2003. Patterning of the lateral ganglionic eminence by the Gsh1 and Gsh2 homeobox genes regulates striatal and olfactory bulb histogenesis and the growth of axons through the basal ganglia. J Comp Neurol 461:151–165.

Zaki PA, Quinn JC, Price DJ. 2003. Mouse models of telencephalic development. Curr Opin Genet Dev 13:423–437.

Zetterberg A, Larsson O, Wiman KG. 1995. What is the restriction point? Curr Opin Cell Biol 7:835–842.

Zhang Z, Swindle CS, Bates JT, Ko R, Cotta CV, Klug CA. 2007. Expression of a non-DNA-binding isoform of Helios induces T-cell lymphoma in mice. Blood 109:2190–2197.